European Journal of Medicinal Chemistry 224 (2021) 113692

Contents lists available at ScienceDirect

European Journal of Medicinal Chemistry

journal homepage: http://www.elsevier.com/locate/ejmech

Optimization of peptide-based inhibitors targeting the HtrA serine protease in Chlamydia: Design, synthesis and biological evaluation of pyridone-based and N-Capping group-modified analogues

Jimin Hwang [a, 1], Natalie Strange [b, 1], Matthew J.A. Phillips [b], Alexandra L. Krause [c], Astra Heywood [d], Allan B. Gamble [a, **], Wilhelmina M. Huston [b, ***], Joel D.A. Tyndall [a, *]

[a] School of Pharmacy, University of Otago, Dunedin, 9054, New Zealand
[b] School of Life Sciences, Faculty of Science, University of Technology Sydney, New South Wales, Australia
[c] Department of Microbiology and Immunology, University of Otago, Dunedin, 9054, New Zealand
[d] Department of Biochemistry, School of Biomedical Sciences, University of Otago, Dunedin, 9054, New Zealand

ARTICLE INFO

Article history:
Received 20 May 2021
Received in revised form
4 July 2021
Accepted 5 July 2021
Available online 7 July 2021

ABSTRACT

The obligate intracellular bacterium *Chlamydia trachomatis* (*C. trachomatis*) is responsible for the most common bacterial sexually transmitted infection and is the leading cause of preventable blindness, representing a major global health burden. While *C. trachomatis* infection is currently treatable with broad-spectrum antibiotics, there would be many benefits of a chlamydia-specific therapy. Previously, we have identified a small-molecule lead compound **JO146** [Boc-Val-Pro-Val^{P}(OPh)$_2$] targeting the bacterial serine protease HtrA, which is essential in bacterial replication, virulence and survival, particularly under stress conditions. **JO146** is highly efficacious in attenuating infectivity of both human (*C. trachomatis*) as well as koala (*C. pecorum*) species *in vitro* and *in vivo*, without host cell toxicity. Herein, we present our continuing efforts on optimizing **JO146** by modifying the N-capping group as well as replacing the parent peptide structure with the 2-pyridone scaffold at P3/P2. The drug optimization process was guided by molecular modelling, enzyme and cell-based assays. Compound **18b** from the pyridone series showed improved inhibitory activity against CtHtrA by 5-fold and selectivity over human neutrophil elastase (HNE) by 109-fold compared to **JO146**, indicating that 2-pyridone is a suitable bioisostere of the P3/P2 amide/proline for developing CtHtrA inhibitors. Most pyridone-based inhibitors showed superior anti-chlamydial potency to **JO146** especially at lower doses (25 and 50 μM) in *C. trachomatis* and *C. pecorum* cell culture assays. Modifications of the N-capping group of the peptidyl inhibitors did not have much influence on the anti-chlamydial activities, providing opportunities for more versatile alterations and future optimization. In summary, we present 2-pyridone based analogues as a new generation of non-peptidic CtHtrA inhibitors, which hold better promise as anti-chlamydial drug candidates.

1. Introduction

Chlamydia trachomatis (C. trachomatis) is one of the most common sexually transmitted bacterial pathogens and a leading cause of preventable blindness worldwide [1,2]. Despite the effectiveness of currently available antibacterial agents for *C. trachomatis*, management of the infection remains challenging with escalating global prevalence. According to the latest World Health Organization (WHO) reports, the reported prevalence of Chlamydia has steadily increased with 92, 101, 131, and 153 million incidences in 2009, 2011, 2012 and 2015, respectively [3,4]. *C. trachomatis* is often seen as a co-infection with *Neisseria gonorrhoeae* or *Mycoplasma genitalium*, which have already developed resistance to macrolides and tetracyclines [5–7]. Thus, designing new antibacterial drugs that specifically target Chlamydia may provide an avenue for reducing the pressure of antibiotic resistance development in other pathogens.

* Corresponding author.
** Corresponding author.
*** Corresponding author.
E-mail addresses: allan.gamble@otago.ac.nz (A.B. Gamble), Wilhelmina.Huston@uts.edu.au (W.M. Huston), joel.tyndall@otago.ac.nz (J.D.A. Tyndall).
[1] Equal contributions.

https://doi.org/10.1016/j.ejmech.2021.113692
0223-5234/

In addition, Chlamydia (specifically *C. pecorum* and *C. pneumoniae*) is a dominant threat to the koala (*Phascolarctos cinereus*), an iconic marsupial in Australia, that is currently at risk of extinction [8]. Traditional broad-spectrum antibiotics used to treat human infections have limited efficacy in koalas, as the antibiotics are detrimental to their unique gut microbiota that digest toxic *Eucalyptus* leaves [9,10]. In addition, chloramphenicol, the main antibiotic treatment for koala, requires a prolonged course (14–28 days) of daily subcutaneous injections to be effective, and is decreasing in availability in the market [11]. Therefore, development of a new class of antibiotics with a more specified range of bacterial target is urgently needed for the koala not only to treat the infection, but also to limit side effects given their unique digestive system.

HtrA (High Temperature Requirement A), an orthologue of *E. coli* DegP, is an evolutionarily well-conserved serine protease-chaperone which plays a vital role in bacterial replication and survival under stress conditions through protein quality control [12]. HtrA in Gram-negative bacteria are usually localised to the periplasm, but are also found on the outer surface of bacteria or in the extracellular matrix for their direct role in bacterial dissemination and virulence [12]. The crucial function and accessible location of bacterial HtrA makes it an attractive target for chemical inhibition. In fact, earlier studies have shown that HtrA in *E. coli* [12], *H. pylori* [13–15] and *C. trachomatis* [16] could be targeted with small molecule inhibitors at a low micromolar range.

In our previous studies, inhibition of *C. trachomatis* HtrA (CtHtrA) by the lead compound **JO146** (**1**; IC_{50} = 12.5 ± 2.94 μM; Fig. 1) during the bacterial mid-replicative phase resulted in the total loss of inclusion vacuoles and lethality of the human, mouse and koala Chlamydia strains *in vitro* and *in vivo* without causing cytotoxicity [16,17]. **JO146** was selective for CtHtrA over other serine proteases including trypsin (IC_{50} > 500 μM) and chymotrypsin (IC_{50} > 500 μM), but not human neutrophil elastase (HNE; IC_{50} 2.24 μM ± 0.12 μM) [16]. Although HtrA proteases are ubiquitous in cells, their structural, functional and mechanistic disparities between Gram-negative, Gram-positive bacteria and mammalian cells make HtrAs a more favourable target for selectivity [12,18].

Herein, **JO146** was optimized by replacing the P3/P2 backbone by a non-peptidic 2-pyridone template. The 2-pyridone class and its derivatives are of particular interest in developing small molecule peptide-mimetic inhibitors against various serine (e.g. HNE [19], HCV NS3/4 A [20], thrombin [21,22] and tissue factor VIIa [23–26]) and cysteine proteases (e.g. human rhinovirus 3C [27,28], COVID-19 M^{pro} (or $3CL^{pro}$) [29] and *P. falciparum* falcipain-2/3 [30]). The non-natural pyridine ring, which masks the P3–P2 amide bond could suppress hydrolytic cleavage by host proteases, potentially alleviating general pharmacokinetic problems (e.g., poor stability and oral bioavailability) associated with peptide-based compounds. In this study, a variety of pyridone analogues were synthesized with different combinations of P1, P2, P3 and the capping group along with a diphenyl phosphonate transition state analogue in a stepwise optimization method. To evaluate the compatibility of different N-capping groups in the S4 pocket of CtHtrA, a small pool of modified groups was also coupled with the new peptidic lead compounds **2** and **3**, which were previously optimized by incorporating unnatural residues at P3 and/or P1 (Fig. 1) [31].

2. Results and discussions

2.1. Synthetic chemistry

2.1.1. 2-Pyridone-based inhibitors

Pyridone analogues were synthesized with different combinations of P1, P2, P3 and capping group residues along with the diphenyl phosphonate warhead group that is responsible for forming an irreversible covalent bond with the catalytic serine residue. Previously, adaptations at the electrophilic warhead group with non-covalent (N-alkyl methylamides, valinol), and reversible, covalent (boronates, α-diketones, α-ketoesters, α-ketoamides and α-ketoheterocycles) transition state analogues (TSA) were investigated for optimization of **JO146** [33]. Although these warhead groups have previously been reported to be active against serine proteases [31,34–39], only α-ketobenzothiazole from the α-ketoheterocycle series was active with comparable CtHtrA inhibition to that by **JO146** [31]. Therefore, covalent inhibition between the inhibitor and the active site of CtHtrA is crucial for anti-chlamydial activity and diphenyl phosphonate remains the most effective warhead group against CtHtrA to date.

The synthesis of the 2-pyridone analogues with modifications of the capping group, P2 and P1 is outlined in Scheme 1. Commercially available 3-nitro-2-pyridone **4** was reduced to 3-amino-2-pyridone **5** in the presence of 10% palladium on carbon under $H_{2(g)}$. The Cbz protection of the aniline in compound **5** was readily achieved by N-acylation with benzyl chloroformate under the Schotten-Baumann conditions [40] to give **6**. However, due to the low reactivity of the aryl amine, Boc protection of pyridone **5** with a NaOH in an aqueous environment was low yielding, regardless of prolonged reaction time (up to 65 h), temperature (up to 55 °C) and addition of a large excess of di-*tert*-butyl dicarbonate (up to 5.3 equiv.). The reaction yield was lower when conducted independently in methanol and THF, and triethylamine as base. Therefore, an alternative method was sought using a combination of 4-dimethylaminopyridine (DMAP) and triethylamine as an alternative base combination to NaOH. The starting material **5** was consumed within 4 h using a previous method by Basel et al. [41] However, owing to the

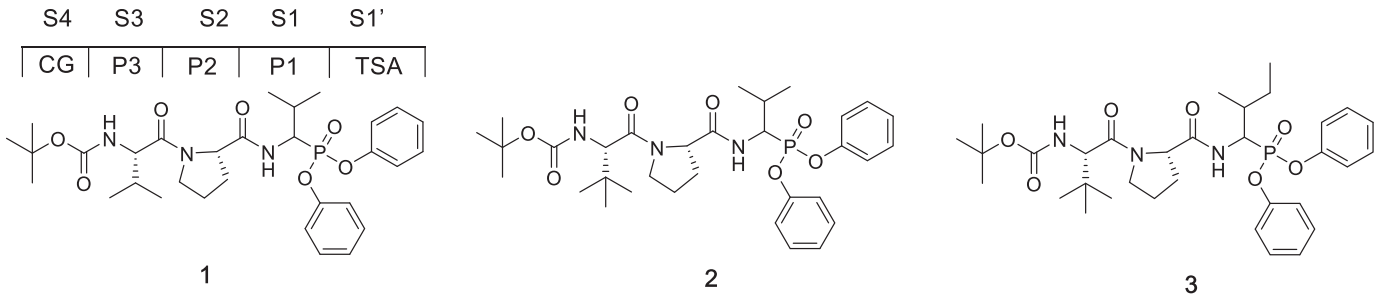

Fig. 1. Structures of the initial lead compound **JO146** (**1**) from high throughput screening [16] and the newer lead compounds **2** and **3** obtained from optimization of P1 and/or P3 residues [31]. Standard nomenclature for peptide substrates in which amino acid residues are denoted as P3–P1 and their corresponding binding subpockets as S4–S1' [32]. TSA – Transition State Analogue. CG – Capping Group.

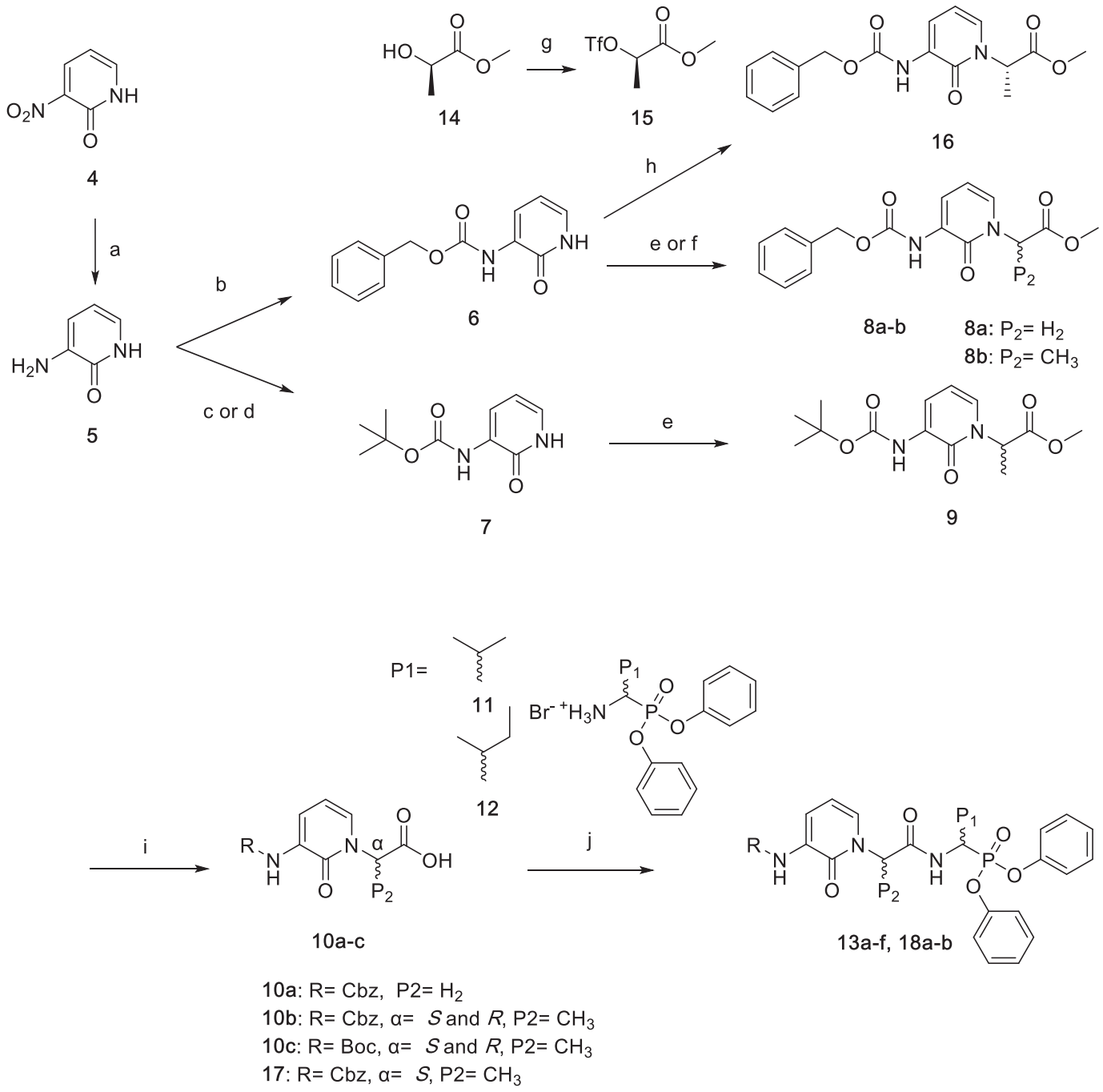

Scheme 1. General Route for the Preparation of Pyridone-based inhibitors.
Reagents and conditions: (a) 10% Pd/C, $H_{2(g)}$, DMF/MeOH, rt, 21 h, 95%; (b) benzyl chloroformate, Na_2CO_3, H_2O/acetone, 0–25 °C, 3 h, 86%; (c) di-*tert*-butyl dicarbonate, NaOH, THF/H_2O, 55 °C, 65 h, 14–21%; (d) di-*tert*-butyl dicarbonate, DMAP, triethylamine, DCM, rt, 4 h, 22%; (e) ethyl iodopropionate, NaH, DMF, 0–25 °C, 3 h, 74%; (f) ethyl iodoacetate, NaH, DMF, 0–25 °C, 3 h, 41–81%; (g) Tf_2O, 2,6-lutidine, CH_2Cl_2, 1 h; (h) NaH, THF, 24 h, 63%; (i) LiOH.H_2O, THF/H_2O, rt, 2 h, 82–98% (j) **11** or **12**, DIPEA, HBTU, DMF, rt, 24 h, 43–79%.

formation of impurities such as N-Boc-urea, urea or isocyanate, as previously reported [41], the yield of **7** remained low (22%).

The N-capped-pyridone-P2 precursors **8a-b** and **9** were synthesized according to the method described by Warner et al. [42] Alanine was incorporated at P2 as a mimic of the C_α-C_β bond in proline. In addition, glycine was added as an alternative to alanine to reduce stereochemical complexity arising from the epimerization of the C_α-P1 chiral centre, which leads to formation of diastereoisomeric mixtures in the final compounds. N-alkylation of compound **6** and **7** was conducted via an S_N2 nucleophilic substitution with α-iodoalkyl esters and NaH to produce **8a-b** and **9** with moderate to high yields 41–81%. Due to the high cost of enantiomerically pure ethyl 2-iodopropionate, a diastereomeric mixture of the reagent was used in the reaction, this theoretically resulted in compound **8b** in both L- and D-alanine (P2). Alternatively, enantiomerically pure (*R*)-lactate **14** was triflated and reacted with compound **6** via S_N2 substitution to produce **16** with an inverted *S*-configuration at P2 [29]. The L-alanine was selected for P2 as it is evolutionarily more abundant and preferred configuration over the D-enantiomer in natural substrates of proteins and proteases.

Compounds **8a-b, 9** and **16** were then converted to free acids by base-catalyzed hydrolysis prior to the P2−P3 peptide coupling with P1-TSA [31] (**11** and **12**) to successfully synthesize **13a-f** and **18a-b**. Our previous studies of P1 optimization showed that replacement of valine by isoleucine resulted in improved anti-CtHtrA potency and selectivity over HNE [31]. Thus, these two hydrophobic residues were investigated in the pyridone series.

All synthesized compounds were characterized by ^{1}H, ^{13}C NMR and mass spectrometry analysis, and produced agreeable spectroscopic data, which were in full accordance with their depicted structures. Diastereomers of the final compounds were further characterized by ^{31}P NMR spectroscopy.

2.1.2. Capping group modification of the peptidic inhibitors

The peptidic lead compounds **JO146**, **2** and **3** were synthesized according to the procedure reported by Agbowuro et al. [31] The tripeptide analogues **28a-28e** were synthesized by a series of solution-phase peptide coupling steps using HBTU coupling reagent in the presence of DIPEA base, and a base-catalyzed hydrolysis of the ester groups (Scheme 2). Cbz protection of *tert*-leucine **19** to provide **20** was achieved by N-acylation with benzyl chloroformate under Schotten-Baumann conditions [40]. A 2:1 M ratio of Na_2CO_3 to $NaHCO_3$ was employed to replace the traditional use of a strong base (NaOH). Using the former provided improved buffering capabilities, hence were preferred to maintain the optimal reaction pH of 8−9 that is required to neutralize the hydrochloric acid formed as a by-product. Neutralizing the acid prevents degradation of the benzyl carbamate in **20**, while avoiding epimerization at the α-amino group with excessive alkalinity.

Replacement of the Boc capping group with *tert*-butyl amide and *tert*-butyl urea was carried out by Boc deprotection of dipeptide **23** using TFA in DCM, and the resulting N-uncapped dipeptide **24** was acylated with *tert*-butyl isocyanate and trimethylacetyl chloride to provide **25** and **26**, respectively. Formation of the *tert*-butyl urea and *tert*-butyl amide capping groups was confirmed by the upfield peak shift of the *tert*-butyl group from 1.41 ppm (**23**) to 1.29 ppm (**25**) and 1.19 ppm (**26**), in accordance with the order of electronegativity of the O, N and C atoms (see NMR spectra in supporting *information*). Given the epimerization-free nature of the Boc deprotection and isocyanate-mediated asymmetric urea formation, duplication of ^{1}H NMR peaks in the *tert*-butyl urea-capped dipeptide ester (**25**) was speculated to be caused by rotamerization. In addition, the replacement of the oxygen in the Boc group by −NH- of the urea accentuates the ability of the amide group to form resonance structures, giving more defined separation of the rotamer peaks of the *tert*-butyl group found in **25** than that in **26**. Rotamerization was verified by the coalescence of deuterated peaks with the NMR solvent change from deuterated chloroform to acetonitrile and variable temperature (Fig. S1).

The key intermediate Cbz-protected α-aminoalkyl diphenyl phosphonates (**11** and **12**) were prepared by the previously described Mannich-type ligation reaction [43] with either 2-methyl butyraldehyde or isobutyraldehyde for valine or isoleucine at P1, respectively [31]. During this reaction, the imine intermediate formed between the benzylcarbamate and aldehyde permits an S_N1 nucleophilic attack by the triphenylphosphite, resulting in both *S* and *R* configurations at the α-aminoalkyl side-chain and the subsequent elimination of a phenoxide group. In the case where 2-methyl butyraldehyde was reacted, an additional chiral centre at C_β of the aminoalkyl sidechain formed both threo (*RR* and *SS*) and erythro (*RS* and *SR*) diastereomers, which were detected by two distinct peaks in the ^{31}P NMR spectrum. The acid-catalyzed Cbz deprotection of N-Cbz-aminoalkyl diphenyl phosphonates by hydrobromide in acetic acid afforded hydrobromide salts of α-aminoalkyl diphenyl phosphonates **11** and **12**. Phosphonates **11** and **12** were then coupled with N-capped-P3-P2 dipeptides **27a-c** and purified by silica gel flash column chromatography to obtain the final compounds **28a-e** in diastereomeric mixtures that were biologically evaluated.

2.2. Enzyme assays

Protease inhibition assays were conducted for compound activity and off-target characterization of the final compounds **13a-f** and **18a-b**. IC_{50} values were measured to assess the inhibitory activities of compounds against CtHtrA and HNE (Table 1). The IC_{50} values varied in different batches of the CtHtrA assays (Table S4A and Table S4B), hence relative potency and selectivity of compounds were determined compared to **JO146** for evaluating their biological activities (Tables 1 and 2) [31]. We believe this variation stems from the requirement for activation of HtrA for optimal enzymatic activity, where recombinant protein may be co-purified with short activating peptides from the expression host which can vary between batches. The assessment of the relative selectivity over HNE compared to **JO146** was particularly important as selectivity between HNE and CtHtrA proteases was unable to be inferred from the IC_{50} derived from the two different assay platforms [44].

Replacement of P2/P3 peptidic backbone with the 2-pyridone template generally resulted in a decrease in the CtHtrA inhibitory potencies relative to **JO146**, as indicated by the diminished IC_{50} values of **13a-f** (Table 1). The analogues with a Boc capping group (**13c** and **13f**) elicited weaker inhibition of CtHtrA than those with the Cbz capping group (**13b** and **13e**), demonstrating the lack of compatibility of the pyridone scaffold with the Boc capping group. These results indicate that concerted modifications, which are conducted with a step-wise approach, at different sites of the lead compounds is necessary to accommodate the three-dimensional change in the inhibitor structure resulting from the insertion of a non-peptidic moiety. Although compounds **13a** and **13d**, both containing glycine at P2, showed weaker inhibition of CtHtrA than **JO146**, their relative selectivity over elastase was improved by approximately 5- and 4-fold, respectively, since the reduction in potency against HNE was greater than CtHtrA. For instance, analogue **13a** reduced inhibitory potency against CtHtrA by half compared to **JO146**, but the IC_{50} difference in elastase assay was significantly greater, by more than 12-fold, resulting in approximately 5-fold improvement in the selectivity relative to **JO146** (Table 1).

Despite the general reduction of anti-CtHtrA inhibition by the pyridone analogues relative to **JO146**, compound **13e** (IC_{50} 19.76 ± 1.19 μM) demonstrated slightly improved inhibitory activity to its corresponding peptide analogue **28e** (IC_{50} 24.88 ± 1.18 μM), which comprises a matching capping group and P1 residue (Table 2). In addition, since the activity of **13e** against HNE decreased by about 20-fold compared to **JO146**, its selectivity towards CtHtrA over HNE was 11-fold greater than **JO146** (Table 1).

Given that **13e** showed the most promising inhibitory and selectivity profile from the pyridone series, compound **18b** was synthesized with L-alanine at P2 and its inhibitory activity against CtHtrA was evaluated separately from the rest of the final compounds (Table S4B). Compound **18b** markedly improved the inhibitory activity against CtHtrA by 5-fold relative to **JO146** (8-fold increase in the relative potency compared to **13e**), implicating a single digit micromolar potency when **JO146** displays the reference IC_{50} value of 12.5 μM reported in literature [16]. Furthermore, its 109-fold improvement in selectivity towards CtHtrA over HNE relative to **JO146** indicates that L-alanine is critical at P2 for biological recognition of CtHtrA in the pyridone series. The marked improvement in the selectivity profile could suggest reduction in off-target toxicity *in vivo*. These results together indicated that

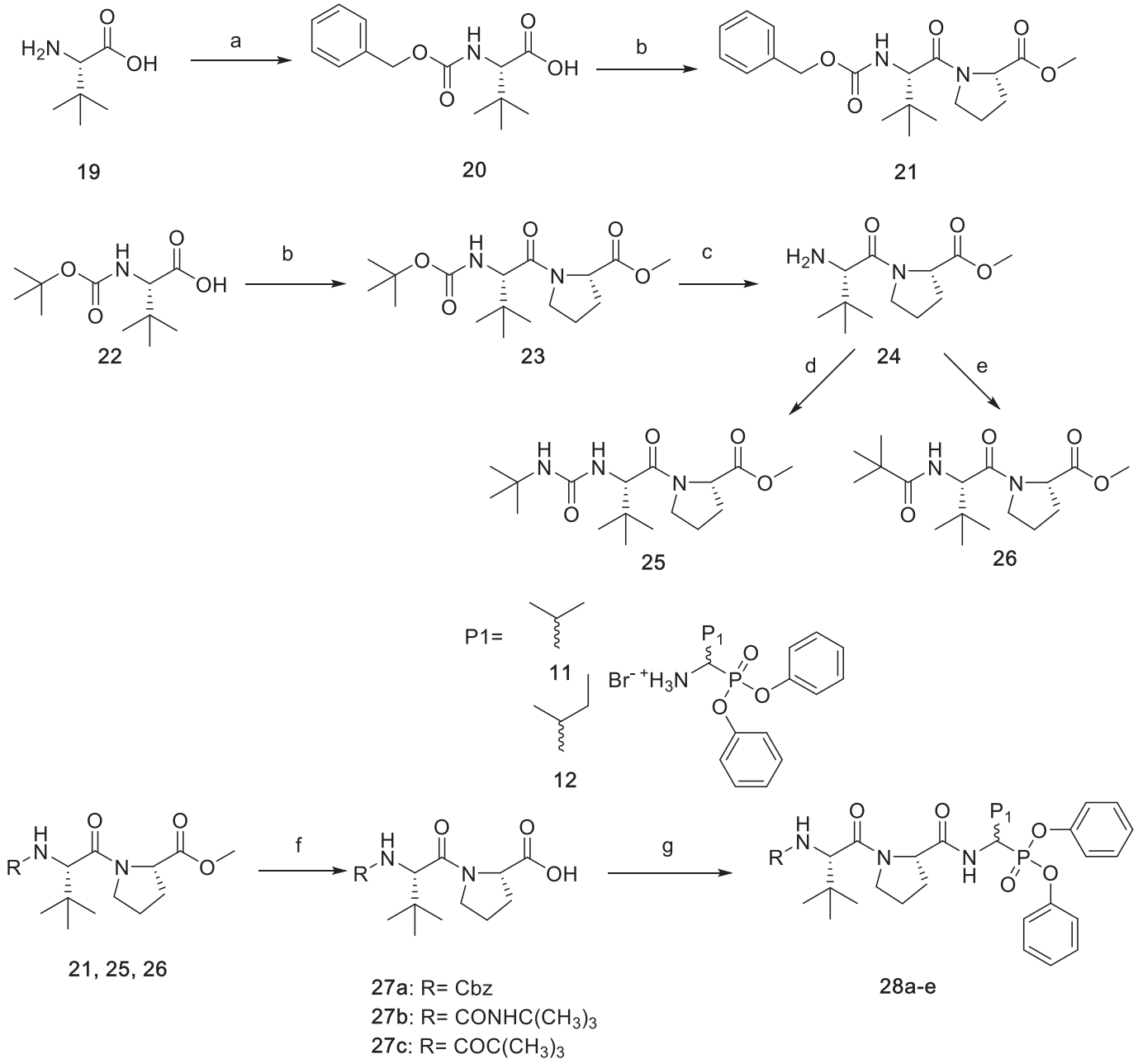

Scheme 2. Functionalization of the N-capping group.
Reagents and conditions: (a) benzyl chloroformate, Na_2CO_3, $NaHCO_3$, H_2O/acetone, rt, overnight, 82%; (b) L-proline methyl ester.HCl, DIPEA, HBTU, DMF, rt, 24 h, 91–100%; (c) TFA, DCM, rt, 2 h, 100%; (d) *tert*-butyl isocyanate, DMF, rt, overnight, 45%, (e) trimethylacetyl chloride, $NaHCO_3$, H_2O/acetone, rt, overnight, 82%; (f) $LiOH.H_2O$, THF/H_2O, rt, 2 h, 91–100%; (g) **11** or **12**, HBTU, DIPEA, DMF, rt, 24 h, 52–82%.

pyridone is a suitable bioisostere for P3/P2 amide, and careful design of pyridone analogues with an optimal combination of the capping group, P2 and P1 could improve binding affinity and selectivity of the parent peptide inhibitors to the active site of CtHtrA.

Variations of the N-capping group had previously been employed in the development of HCV NS3/4A serine protease inhibitors, which allowed improvement in the enzymatic inhibition and selectivity against HNE [45]. Here, modifications of the capping group displayed similar anti-CtHtrA activity to the lead compounds (**JO146**, **2** and **3**; Table 2). Of the three analogues with a Tle-Pro-Val peptide backbone, the compounds with a Boc (**2**) and Cbz (**28d**) protecting group performed equally well, closely followed by *tert*-butyl urea capping group (**28b**). Compounds with Ile at P1 generally decreased anti-CtHtrA potency compared to those with Val at P1 with matching capping groups. Among compounds with Ile at P1, replacement of the Boc capping group by *tert*-butyl urea (**28c**) or Cbz (**28e**) did not compromise the inhibitory activity against CtHtrA compared to their corresponding lead compound **3**. Analogue **28a** with a *tert*-butyl amide capping group, on the other hand, increased the anti-CtHtrA activity approximately 3-fold and the relative selectivity to almost 18-fold relative to **JO146** (Table 2). Inhibitor **28a** was also still slightly better in relative potency (more than 2-fold) and selectivity (1.3-fold) compared to **3**, which share the

Table 1
Inhibitory activities (IC_{50}) of pyridone inhibitors **13a-f** and **18a-b** in CtHtrA and HNE enzyme assays.

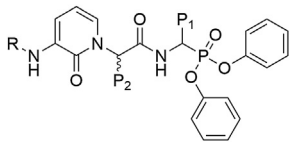

Cmpd	R	P2	P1	IC_{50} ± SEM (μM)		Relative selectivity[c]
				CtHtrA (Relative inhibition against CtHtrA[a])	HNE (Relative inhibition against HNE[b])	
JO146	Boc	Pro	Val	12.47 ± 1.11 (1)	1.15 ± 0.10 (1)	1
13a	Cbz	Gly	Val	28.98 ± 1.21 (0.43)	12.81 ± 0.54 (0.09)	4.79
13b	Cbz	L,D-Ala	Val	41.77 ± 1.31 (0.30)	3.60 ± 0.36 (0.32)	0.93
13c	Boc	L,D-Ala	Val	76.98 ± 1.23 (0.16)	6.64 ± 0.22 (0.17)	0.94
13d	Cbz	Gly	Ile	48.34 ± 1.18 (0.26)	16.48 ± 2.25 (0.07)	3.70
13e	Cbz	L,D-Ala	Ile	19.76 ± 1.19 (0.63)	21.47 ± 3.97 (0.05)	11.8
13f	Boc	L,D-Ala	Ile	128.5 ± 1.16 (0.10)	13.37 ± 0.67 (0.09)	1.03
18a	Cbz	L-Ala	Val	NA	6.01 ± 0.48 (0.19)	NA
18b	Cbz	L-Ala	Ile	(5.07)[d]	24.97 ± 4.72 (0.05)	109

IC_{50} data presented as mean values for triplicates (n = 3).
NA-not assessed.
[a] Relative inhibition against CtHtrA is the ratio of $IC_{50\ CtHtrA}$(**JO146**) to $IC_{50\ CtHtrA}$ (compound).
[b] Relative inhibition against HNE (rounded to 2 decimal place) is the ratio of $IC_{50\ HNE}$ (**JO146**) to $IC_{50\ HNE}$ (compound).
[c] Relative selectivity (rounded to 3 significant figure) towards CtHtrA over HNE is the ratio of the relative potency against CtHtrA to relative potency against HNE compared to that of **JO146**.
[d] Table S4B.

Table 2
Inhibitory activities (IC_{50}) of compounds **28a-e** in CtHtrA and HNE enzyme assays.

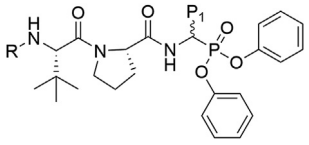

Cmpd	R	P1	IC_{50} ± SEM (μM)		Relative selectivity[c]
			CtHtrA (Relative inhibition against CtHtrA[a])	HNE (Relative inhibition against HNE[b])	
JO146	Boc	Val	12.47 ± 1.11 (1)	1.15 ± 0.10 (1)	1
2	Boc	Val	9.30 ± 1.10 (1.34)	3.02 ± 0.18 (0.38)	3.52
3	Boc	Ile	10.26 ± 1.17 (1.22)	13.51 ± 0.81 (0.09)	14.28
28a		Ile	4.57 ± 1.21 (2.73)	7.69 ± 1.12 (0.15)	18.23
28b		Val	10.65 ± 1.17 (1.17)	1.17 ± 0.17 (0.98)	1.20
28c		Ile	14.09 ± 0.89 (0.89)	5.66 ± 1.08 (0.03)	4.44
28d		Val	9.30 ± 1.18 (1.34)	1.35 ± 0.25 (0.11)	1.74
28e		Ile	24.88 ± 0.50 (0.50)	2.47 ± 0.11 (0.47)	1.11

IC_{50} data presented as mean values for triplicates (n = 3).
[a] Relative inhibition against CtHtrA (rounded to 2 decimal place) is the ratio of $IC_{50\ CtHtrA}$(**JO146**) to $IC_{50\ CtHtrA}$ (compound).
[b] Relative inhibition against HNE (rounded to 2 decimal place) is the ratio of $IC_{50\ HNE}$ (**JO146**) to $IC_{50\ HNE}$ (compound).
[c] Relative selectivity (rounded to 3 significant figure) towards CtHtrA over HNE is the ratio of the relative potency against CtHtrA to relative potency against HNE compared to that of **JO146**.

same P1 and P3 amino acid residues. Based on the assay results, the oxygen atom placed between the carbonyl and *tert*-butyl group in the parent Boc capping group is not necessary for interacting with the target peptide backbone, hence removing it (**28a)** or replacing it

by a hydrogen bond donor (**28b-c**) did not affect the anti-CtHtrA potency. In fact, since the S4 pocket is shallow and exposed to the solvent environment, it could accommodate longer and bulkier capping groups such as the carboxybenzyl group (**28d-e**). This supports the observation that the Cbz group was indeed an appropriate capping group for the 2-pyridone inhibitors. In addition, these results showed that the capping group could be an opportunistic site to add further functionality with different physicochemical properties to the Boc group, which might be able to alleviate the solubility issue inherent with the hydrophobic inhibitor **JO146** [46].

2.3. Anti-bacterial and cytotoxicity cell assays

2.3.1. JO146 has a narrow anti-bacterial specificity

Despite HtrA proteases being widely expressed in bacteria, the domain architecture varies between Gram-negative and Gram-positive bacteria [18]. **JO146** and the new lead compounds **2** and **3** completely lacked inhibitory activity against *Pseudomonas aeruginosa* (at 50 and 100 μM), *Staphylococcus aureus* and *Escherichia coli* (at 50 μM), supporting that this class of covalent inhibitors is specific for Chlamydial HtrA or at least have a very narrow spectrum of bacterial target even within one Gram stain grouping (Figs. S4 and S5 and Tables S5 and S6). These results indicate that although HtrA is ubiquitous in bacteria, structural and functional differences between species could allow fine-tuning of target specificity. Identification and development of such pathogen-specific antibacterial reagents that target only one or a small set of species would be highly valuable in clinical use for their potential in minimizing disturbance of the host microbiome and slowing the spread of resistance [47].

2.3.2. 2-pyridone inhibitors

The *in vitro* potency of all compounds was assessed by their ability to significantly reduce the number of inclusion-forming units (IFU/mL; Tables S1 and S2) of *C. trachomatis* and *C. pecorum* isolates in cell culture, which is a traditional quantitative measure of the pathogen's infectivity or transmissibility [48]. It is noteworthy that the bacterial titre of the control group was about 10^4 lower in *C. pecorum* assays than *C. trachomatis* as the former isolate is more cytotoxic to host cells *in vitro*, which limits the number of infectious progeny able to be cultured.

Pyridone analogues, including those that showed decreased CtHtrA activities relative to **JO146**, showed overall improvement in the anti-bacterial activities compared to **JO146** especially at 25 μM in both *C. trachomatis* and *C. pecorum* isolates (Fig. 2). These results could suggest that the pyridone analogues might have a different or secondary mechanism of anti-chlamydial action other than inhibiting the CtHtrA protease.

Compounds **13d-f**, which share isoleucine at P1 and inhibited *C. trachomatis* more effectively at 25 μM than compounds **13a-c** with valine at P1. Compounds **13d-f** on average resulted in approximately 3.7-log further reduction in the IFU/mL count than **JO146** at 25 μM. On the other hand, **13a-c** displayed stronger anti-chlamydial activities at 50 and 100 μM doses. In particular, **13c** showed a good dose-response relationship and decreased the bacterial titre below the lower limit of detection at 100 μM. In *C. pecorum* assays, the pyridone analogues were more effective in reducing the bacterial titre compared to **JO146**. All compounds diminished the infectious progeny close to the limit of detection even at 25 μM except **13c**.

Compounds **18a** and **18b** were more potent than **JO146** against *C. trachomatis* by approximately a log and 1.6-log difference in IFU/

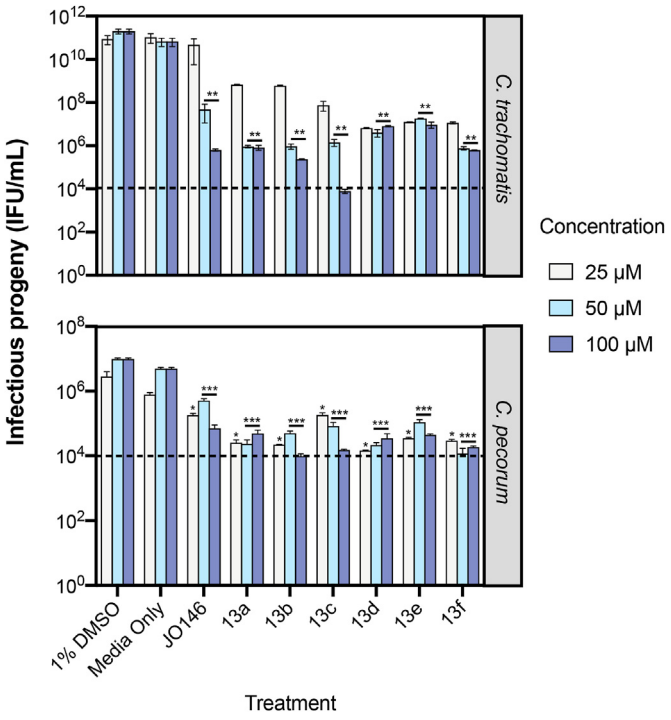

Fig. 2. *In vitro* testing of *Chlamydia trachomatis* and *C. pecorum* growth inhibition by the lead compound **JO146** and pyridone analogues **13a-f** at 25, 50 and 100 μM. Dashed line indicates the limit of detection for inclusion forming units (IFU). Error bars represent the SEM (n = 3). **p*-value <0.05, ***p*-value <0.001, ****p*-value <0.0001 compared to DMSO control as measured by two-way ANOVA.

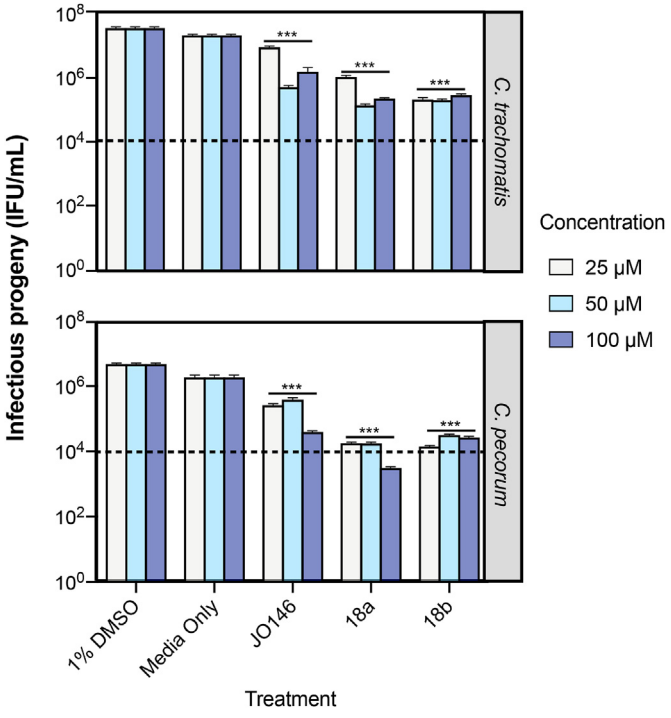

Fig. 3. *In vitro* testing of *Chlamydia trachomatis* and *C. pecorum* growth inhibition by the lead compound **JO146** and pyridone analogues **18a** and **18b** at 25, 50 and 100 μM. Dashed line indicates the limit of detection for inclusion forming units (IFU). Error bar represents the SEM (n = 3). ****p*-value <0.0001 compared to DMSO control as measured by two-way ANOVA.

mL, respectively, at 25 μM. In *C. pecorum* assays, both compounds obliterated the infectious progeny to the limit of detection even at 25 μM (Fig. 3).

Overall, the replacement of the traditional peptidic structure by the new pyridone scaffold produced compounds that exhibited improved inhibitory action against Chlamydia, therefore further optimization of this class of inhibitors is worthwhile.

Cytotoxicity of the pyridone analogues on the human epithelial (HEp-2) cells was assessed by MTS cell viability and LDH cytotoxicity assays, which represent the level of cellular metabolism and proliferation (as markers of cell viability), and cellular integrity (as a marker of cell lysis and death), respectively (Fig. 4). All pyridone-based analogues resulted in a non-cytotoxic relative reduction in MTS absorbance of ≤25% at 25 and 100 μM concentration (Fig. 4a). Standardised international guidelines for testing cytotoxicity suggest that cell viabilities <70% are indicative of cytotoxic potential; none of the compounds tested affected cell viability to this degree [49,50]. Compound **13f** had a statistically significant effect on host cell integrity at 100 μM concentration, however, this was a relative decrease in cell integrity of <10% (Fig. 4b). These results altogether demonstrated that pyridone analogues were non-cytotoxic to HEp-2 cells and their anti-bacterial efficacy was specific to Chlamydia.

2.3.3. Capping group-modified peptidic inhibitors

All compounds from the capping group series demonstrated improved anti-chlamydial activities relative to **JO146**, except **28e** at 100 μM (Fig. 5). Compounds **28b** and **28d** containing valine at P1 displayed similar anti-chlamydial activities to their lead compound **2**. Despite showing the highest anti-CtHtrA activity (Table 2) within the capping group series, **28a** was the least effective in reducing the bacterial titre at 25 μM with approximately 3.6-log increase in the IFU/mL count of *C. trachomatis* compared to the lead compound **3** with a matching P1 valine. Complementing the enzymatic assay (Table 2), **28e** showed the weakest anti-chlamydial potency at 100 μM against both *C. pecorum* and *C. trachomatis* owing to a poor dose-response correlation. This indicated that the Cbz capping group and Ile at P1 are not complementary to each other in the tripeptidic analogues. The compounds were all effective against *C. pecorum*, reducing the infectious progeny close to the limit of detection (10^4 IFU/mL) at the three doses. Modifications of the N-capping group did not significantly affect the anti-chlamydial potency in *C. pecorum*, similar to the pattern observed in the CtHtrA assays (Fig. 5).

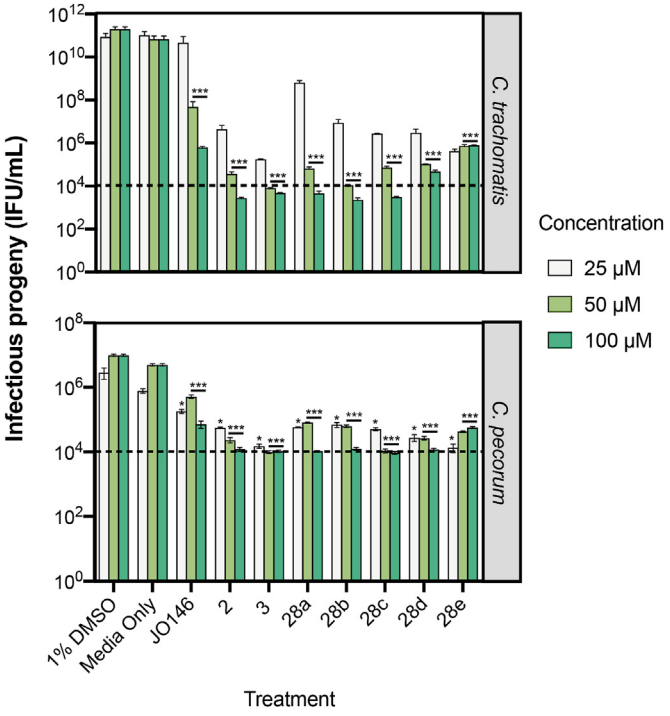

Fig. 5. *In vitro* testing of *Chlamydia trachomatis* and *C. pecorum* growth inhibition by the lead compounds **JO146**, **2** and **3**, and capping group-modified peptide analogues **28a-e** at 25, 50 and 100 μM. Dashed line indicates the limit of detection for inclusion forming units (IFU). Error bar represents the SEM (n = 3). **p*-value <0.05, ****p*-value <0.0001 compared to DMSO control as measured by two-way ANOVA.

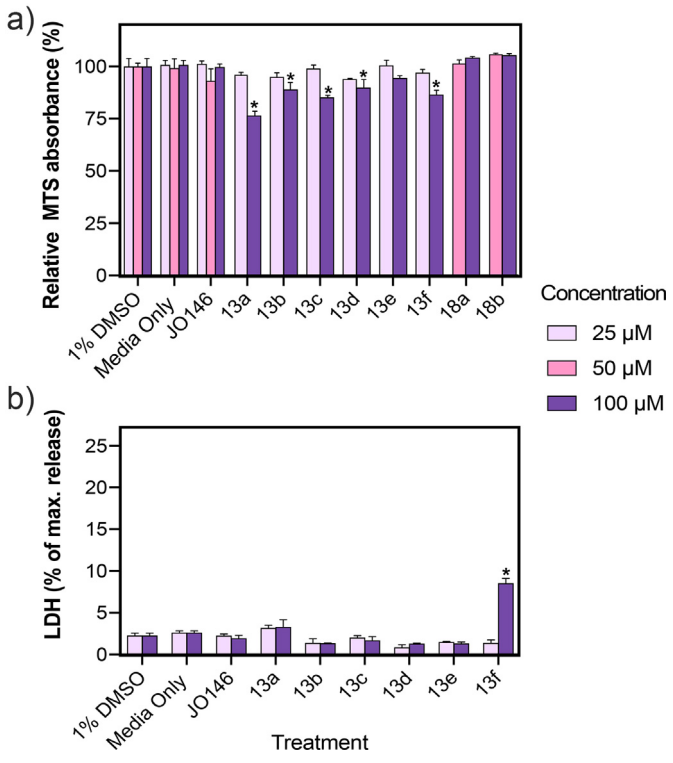

Fig. 4. Viability and integrity of HEp-2 cells treated with pyridone-based analogues. (top) The percentage of MTS reduction compared to cells treated with 1% DMSO. (bottom) The percentage of extracellular LDH detected compared to maximum release controls. Error bars represent the SEM (n = 3). **p*-value <0.05 compared to DMSO controls as measured by two-way ANOVA.

All compounds of the capping group series (**28a-e**) were non-cytotoxic to HEp-2 cells at 25 μM but had a statistically significant effect on cell metabolism when added at 100 μM concentration (Fig. 6a). It is noteworthy that compound **28e**, which demonstrated a poor inhibitory activity against CtHtrA and a lack of dose-dependent efficacy in Chlamydial cell inhibition assays, reduced relative MTS absorbance by approximately 22% even at 25 μM. These biological results suggest that the Cbz capping group is not favoured with a peptidyl inhibitor containing isoleucine at P1. Nevertheless, cell integrity was not impacted as indicated by the level of extracellular LDH release being ≤3.4% for all compounds at both doses (Fig. 6b). The slightly contrasting results of the cytotoxicity profile of the capping group analogues at 100 μM between the MTS and LDH assays can be explained by the difference in the cellular processes or markers the assays measure. Given that MTS assay measures the level of tetrazolium reduction to formazan in actively metabolizing or proliferating cells, MTS reduction does not directly translate to cell death and can even be reversible upon elimination of the inhibitors. In contrast, the level of cytosolic LDH leakage indicates the loss of cell integrity and cell lysis, which

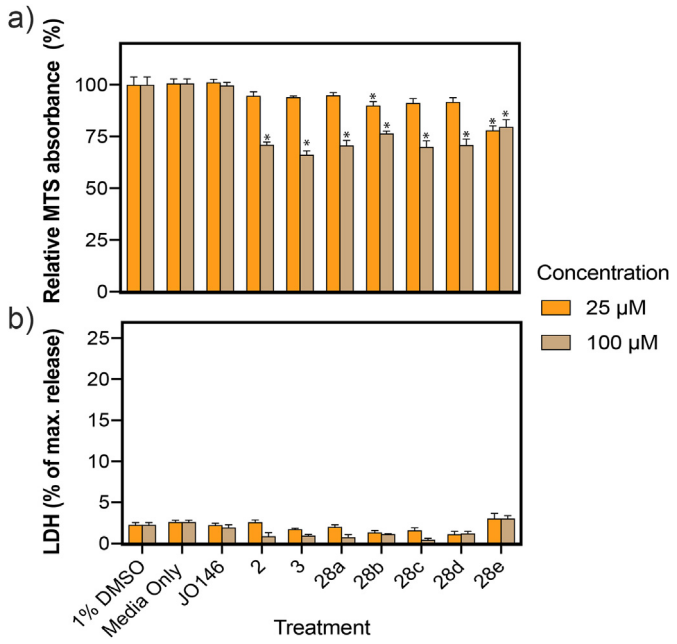

Fig. 6. Viability and integrity of HEp-2 cells treated by lead compounds **JO146**, **2** and **3**, and capping group-modified peptide analogues **28a-e** (analogues of the structure R-Tle-Pro-P1^{P}(OPh)$_2$). Error bars represent the SEM (n = 3). **(top)** The percentage of MTS reduction compared to cells treated with 1% DMSO. (bottom) The percentage of extracellular LDH detected compared to maximum release controls. *Significantly different (p-value <0.05) from DMSO controls as measured by two-way ANOVA.

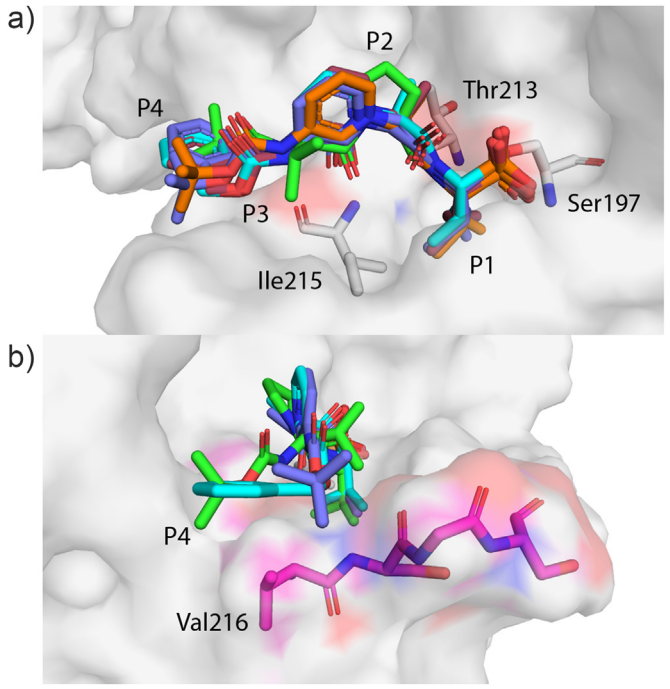

Fig. 7. Docking of 2-pyridone analogues in comparison to **JO146** (green) at the active site of CtHtrA protease. (top) 2-pyridone-based compounds (**13a-f**; those with alanine at P2 were docked with L-configuration) and **JO146** (green) were docked into the active site of CtHtrA. Two H-bond constraints were used in the docking. (bottom) Side view from the N-terminus of **JO146** (green), **13b** (cyan) and **13c** (purple) docked with L-configuration of alanine (P2) into the active site of CtHtrA. The outer wall of the S3 pocket (Val216-Ser219) is highlighted in magenta.

indicates irreversible cell death. Therefore, the results all together point towards the fact that these compounds were not cytotoxic to HEp-2 cells but affected aspects of cellular metabolism at 100 μM at the point of time the measurements were taken.

2.4. Molecular modelling

2.4.1. In silico docking studies of 2-pyridone-based inhibitors

The 2-pyridone-based analogues were covalently docked into the homology model of CtHtrA [51] and compared to the lead compound **JO146**. For the ligands synthesized as racemic mixtures of alanine at the P2 position, the L-enantiomer was docked and analysed. Compounds with glycine and L-alanine at P2 bound to the active site of CtHtrA with high topological similarity to **JO146**, indicating that the 2-pyridone scaffold was a successful isosteric replacement of the traditional peptidic structures. In addition, the methylene bridge of glycine at the P2 position of **13a** and **13d** was perfectly aligned with the superimposed peptide backbone of **JO146** (Fig. 7a). These results were expected as previous X-ray crystallography studies showed that 2-pyridone inhibitors of serine proteases were capable of forming a stable, tetrahedral, hemiketal adduct covalently linked to the catalytic serine, and inducing an extended β-strand conformation while retaining hydrogen bond interactions present in the proteases' natural substrates [25,42,52].

There was slight discrepancy in the position of the N-Boc capping group between 2-pyridone ligands and **JO146**. Compared to the peptidic analogues exemplified by **JO146**, which positioned the Boc group deep into the S4 pocket, the N-Boc group of the pyridone analogues was positioned towards the outer wall (Fig. 7b) of the S4 pocket. This can be explained by the fact that the sp^2-hybridised C3 of the pyridone (in contrast to the sp^3-hybridised C_α in a peptidic backbone) positioned the −NH amide group in a planar orientation, away from the S4 pocket (Fig. 7b). The altered positioning of the N-Boc group increased the distance between the −NH of pyridone and the C═O of Ile215 of the protease, preventing the formation of a hydrogen bond that is important for binding at the active site (Table S7). This result may explain the drastic reduction of the anti-CtHtrA activity of **13f** (128.5 ± 14.21 μM), indicating that the Boc N-capping group contributes to the sub-optimal binding affinity to the active site. In contrast, the flexible methylene spacer of the Cbz allows for the benzyl group to move towards the S4 pocket, maintaining hydrophobic interactions with Val216 at the S4 pocket (Fig. 7b). These results complement the IC_{50} assays (Table 1) that **13b** and **13e** with the Cbz capping group demonstrating superior anti-CtHtrA activities over **13c** and **13f** with the Boc group.

3. Conclusions

In comparison to peptide-based inhibitors that are generally characterized with poor pharmacokinetic profiles due to their inherent instability, peptidomimetics are considered advantageous in reducing susceptibility to proteolytic degradation as well as resistance development in bacteria [53]. Herein, 2-pyridone-based peptidomimetics were designed to replace the P2/P3 peptidic structure of the lead compound **JO146**, which inhibits HtrA serine protease in Chlamydia. The lack of anti-bacterial activity of **JO146** against *E. coli*, *P. aeruginosa* and *S. aureus* highlighted its merit of being a narrow spectrum anti-bacterial, which would reduce selection for anti-bacterial resistance and the detrimental effect upon the host microbiome. Compound **18b** from the pyridone series improved inhibitory activity against CtHtrA by 5-fold and selectivity over HNE by over 100-fold relative to **JO146**. Pyridone-based inhibitors with L,D-alanine at P2 generally elicited lower anti-CtHtrA activities than **JO146**, underlining the significance of L-

configuration of alanine. Compounds **13a** and **13d** were designed with replacement of alanine by glycine at P2 in an attempt to reduce stereochemical complexity of the inhibitors. Although glycine at P2 was less favourable than L-alanine, it was still compatible with the pyridone structure with improvement of selectivity over HNE relative to **JO146**. The pyridone analogues generally exhibited greater anti-chlamydial activity on whole cells especially at 25 and 50 μM, supporting 2-pyridone as a suitable and biologically active template for targeting Chlamydia. The pyridone inhibitors were non-cytotoxic to HEp-2 cells unlike the peptide-based analogues, all of which significantly reduced the relative MTS levels at 100 μM. Modifications of the capping group of the parent peptidic structures suggested flexibility of the S4 pocket in accommodating more diverse structures, providing avenues to improve physicochemical properties of the lipophilic inhibitors in future optimization. Overall, the N-Cbz-2-pyridone moiety was found to be a potential bioisostere for the traditional 'N-capped-P3-P2' peptide structure, which provides an alternative approach for future drug optimization in developing anti-chlamydial drugs.

4. Experimental

4.1. Chemistry

4.1.1. General methods

All solvents and reagents were commercially procured (Sigma-Aldrich, Merck, AK Scientific, Thermo Scientific, Acros Organics, BDH, and Cambridge Isotope) and used without further purification. Organic solvent extracts were dried with $MgSO_{4(s)}$ and subjected to rotary evaporation, and finally dried at 10^{-1} mbar using a high vacuum pump. Silica gel 60 (0.040–0.063 mm, 200–400 mesh) was used for flash column chromatography with all solvent systems expressed as volume to volume (v/v) ratios. Solids were recrystallized from a minimum amount of hot solvent and collected by vacuum filtration. Analytical thin layer chromatography (TLC) was performed on Merck TLC aluminium plates coated with 0.2 mm silica gel 60 F254. Spots were generally detected by UV (254 nm) and/or permanganate staining. ^{1}H, ^{13}C and ^{31}P NMR spectra were recorded at room temperature on Varian 400 or 500 MHz spectrometers. Samples were prepared in deuterated solvents, chloroform (δ 7.26, 77.16 ppm), methanol (δ 3.31, 49.00 ppm) or acetonitrile (δ 1.95, 118.69 and 1.72 ppm) with the respective ^{1}H and ^{13}C chemical shifts shown in brackets. Chemical shifts (δ) are expressed in parts per million (ppm) and coupling constants (J) in Hertz (Hz), both measured against the residual solvent peak. High resolution mass spectrometry was recorded on a Bruker microTOF-Q spectrometer with an electrospray ionization (ESI) source. The purity of compounds was determined by reverse-phase high performance liquid chromatography (HPLC) carried out on an Agilent HPLC with a Gemini 5 μm C18 110 column (250 Å ~4.6 mm, Phenomenex, New Zealand). Compounds were eluted using solvent A: 0.1% trifluoroacetic acid (TFA) in water and solvent B: 0.1% TFA in acetonitrile (ACN) over a linear gradient according to the methods specified (supporting *information*). Compounds were detected at 254/210 nm with a flow rate of 1.0 mL/min. Optical rotation was recorded by using an Autopol IV polarimeter (Rudolph Research Analytical, USA). Final compounds including those obtained as isomeric mixtures, are >95% pure, see supporting information for HPLC traces of the compounds.

4.1.2. Synthesis and characterization of final compounds ***13a-f***, ***18a-b***, ***28a-e***

Synthetic procedures and characterization of precursor compounds (**8**–**10**, **15**–**17**, **20**, **21**, **23**–**27**) are reported in the supporting *information.*

General procedure for peptide coupling to α-aminoalkyl phosphonate diphenyl esters (13a-f, 18a-b, 28a-e). To the solution of a hydrobromide salt of 1-aminoalkyl phosphonate diphenyl ester **11** or **12** (1.5 equiv.) in anhydrous DMF was added DIPEA (2.5 equiv.), and the reaction mixture was stirred for 10 min until complete dissolution was achieved. The acid precursor (1.0 equiv.) in anhydrous DMF was then added dropwise, followed by the addition of HBTU (1.2 equiv.). The reaction mixture was stirred at room temperature for 24 h. When the reaction was complete, the mixture was extracted with EtOAc (3 × 25 mL) and the combined organic layers were washed with saturated aqueous $NaHCO_3$ (3 × 25 mL), MilliQ water (3 × 25 mL) and then brine (3 × 25 mL). The organic layer was dried over $MgSO_{4(s)}$, filtered, concentrated *in vacuo* then purified by flash column chromatography (3:2 Hex:EtOAc).

Phenyl N-[1-({[1-(diphenoxyphosphoryl)-2-methylpropyl]carbamoyl}methyl)-2-oxo-1,2-dihydropyridin-3-yl]carbamate (13a). Compound **11** (0.24 g, 0.63 mmol), **10a** (0.19 g, 0.63 mmol), DIPEA (270 μL, 1.57 mmol), HBTU (0.29 g, 0.76 mmol) in DMF (2 mL) were reacted and purified as described in the general procedure above using to yield a colourless oil **13a** as a racemic mixture (0.30 g, 0.50 mmol, 79%, R_f 0.31, 1:1 Hex:EtOAc). $[\alpha]_{589}^{21} = -2.38$ (c = 0.6, $CHCl_3$). ^{1}H NMR (400 MHz, $CDCl_3$) δ 8.08 (d, J = 7.6 Hz, 1H), 7.80 (s, 1H), 7.57 (d, J = 10.0 Hz, 1H), 7.38–7.05 (m, 15H), 6.98 (dd, J = 6.8, 1.6 Hz, 1H), 6.28 (t, J = 7.2 Hz, 1H), 5.17 (s, 2H), 4.71–4.63 (m, 2H), 4.53–4.49 (m, 1H), 2.45–2.35 (m, 1H), 1.08–1.01 (m, 6H). ^{13}C NMR (101 MHz, $CDCl_3$) δ 167.0 (d, $J_{C\text{-}P}$ = 6.1 Hz), 157.3, 153.2, 150.1 (d, $J_{C\text{-}P}$ = 10.5 Hz), 149.9 (d, $J_{C\text{-}P}$ = 9.5 Hz), 135.7, 129.8 (d, $J_{C\text{-}P}$ = 0.9 Hz), 129.7 (d, $J_{C\text{-}P}$ = 0.8 Hz), 129.50, 128.6, 128.4, 128.3, 125.4 (d, $J_{C\text{-}P}$ = 1.1 Hz), 125.2 (d, $J_{C\text{-}P}$ = 1.0 Hz), 121.1, 120.6 (d, $J_{C\text{-}P}$ = 4.1 Hz), 120.3 (d, $J_{C\text{-}P}$ = 4.4 Hz), 107.7, 67.2, 54.0, 51.4 (d, $J_{C\text{-}P}$ = 154.4 Hz), 50.6, 29.1 (d, $J_{C\text{-}P}$ = 3.7 Hz), 20.4 (d, $J_{C\text{-}P}$ = 13.4 Hz), 17.9 (d, $J_{C\text{-}P}$ = 4.8 Hz). ^{31}P NMR (162 MHz, $CDCl_3$) δ 16.49. HRMS-ESI calculated for $C_{31}H_{32}N_3NaO_7P$ [M + Na^+] 612.1870, found *m/z* 612.1842. Analytical RP-HPLC (Method I) t_R = 27.57 min.

Phenyl N-[1-(1-{[1-(diphenoxyphosphoryl)-2-methylpropyl]carbamoyl}ethyl)-2-oxo-1,2-dihydropyridin-3-yl]carbamate (13b). Compound **12** (0.27 g, 0.88 mmol), **10b** (0.25 g, 0.80 mmol), DIPEA (350 μL, 2.00 mmol), HBTU (0.36 g, 0.96 mmol) in DMF (2 mL) were reacted and purified as described in the general procedure above to yield a colourless oil **13b** in a diastereomeric mixture (0.30 g, 0.50 mmol, 62%, R_f 0.42, 1:1 Hex:EtOAc). $[\alpha]_{589}^{21} = -1.64$ (c = 0.6, $CHCl_3$). ^{1}H NMR (400 MHz, $CDCl_3$) δ 8.07 (d, J = 7.2 Hz, 0.5H), 7.98 (d, J = 7.2 Hz, 0.5H), 7.89 (s, 0.5H),7.81 (s, 0.5H), 7.70–7.62 (m, 1H), 7.41–7.04 (m, 15H), 6.99–6.96 (m, 0.5H), 6.94–6.91 (m, 0.5H), 6.34 (t, J = 7.2 Hz, 0.5H), 6.22 (t, J = 7.2 Hz, 0.5H), 5.85 (q, J = 7.2 Hz, 0.5H), 5.56 (q, J = 7.2 Hz, 0.5H), 5.20 (s, 1H), 5.13 (s, 1H), 4.69–4.60 (m, 1H), 2.44–2.30 (m, 1H), 1.66 (d, J = 7.2 Hz, 1.5H), 1.54 (d, J = 7.2 Hz, 1.5H), 1.18–1.09 (m, 4H), 0.94–0.91 (m, 1H), 0.81–0.79 (m, 1H). ^{13}C NMR (101 MHz, $CDCl_3$) δ 169.6 (d, $J_{C\text{-}P}$ = 6.1 Hz), 157.5, 157.4, 153.5, 153.3, 150.6 (d, $J_{C\text{-}P}$ = 9.6 Hz), 150.5 (d, $J_{C\text{-}P}$ = 9.8 Hz), 150.2 (d, $J_{C\text{-}P}$ = 9.6 Hz), 150.0 (d, $J_{C\text{-}P}$ = 9.3 Hz), 149.9 (d, $J_{C\text{-}P}$ = 10.2 Hz), 135.97, 135.92, 130.0 (d, $J_{C\text{-}P}$ = 1.0 Hz), 129.90, 129.85 (d, $J_{C\text{-}P}$ = 0.7 Hz), 129.8 (d, $J_{C\text{-}P}$ = 1.1 Hz), 129.74 (d, $J_{C\text{-}P}$ = 0.9 Hz), 129.22, 129.16, 128.8, 128.7, 128.6, 128.5, 128.38, 128.35, 125.5 (d, $J_{C\text{-}P}$ = 1.0 Hz), 125.42 (d, $J_{C\text{-}P}$ = 1.0 Hz), 125.38 (d, $J_{C\text{-}P}$ = 0.8 Hz), 125.34 (d, $J_{C\text{-}P}$ = 1.0 Hz), 125.30 (d, $J_{C\text{-}P}$ = 0.7 Hz), 125.26 (d, $J_{C\text{-}P}$ = 0.9 Hz), 125.2, 125.1, 120.8 (d, $J_{C\text{-}P}$ = 4.1 Hz), 120.73 (d, $J_{C\text{-}P}$ = 4.2 Hz), 120.69 (d, $J_{C\text{-}P}$ = 4.3 Hz), 120.6 (d, $J_{C\text{-}P}$ = 5.2 Hz), 120.46 (d, $J_{C\text{-}P}$ = 4.3 Hz), 120.45 (d, $J_{C\text{-}P}$ = 4.4 Hz), 107.74, 107.72, 67.4, 67.2, 53.9, 53.7, 51.6 (d, $J_{C\text{-}P}$ = 153.0 Hz), 51.5 (d, $J_{C\text{-}P}$ = 155.7 Hz), 29.23 (d, $J_{C\text{-}P}$ = 3.7 Hz), 29.19 (d, $J_{C\text{-}P}$ = 3.8 Hz), 20.7 (d, $J_{C\text{-}P}$ = 12.9 Hz), 20.7 (d, $J_{C\text{-}P}$ = 12.9 Hz), 20.4 (d, $J_{C\text{-}P}$ = 13.6 Hz), 18.4 (d, $J_{C\text{-}P}$ = 5.3 Hz), 17.7 (d, $J_{C\text{-}P}$ = 4.8 Hz), 15.7, 15.3. ^{31}P NMR (162 MHz, $CDCl_3$) δ 17.22 (13.5%), 16.29 (86.5%). HRMS-ESI calculated for $C_{32}H_{34}N_3NaO_7P$ [M + Na^+]

626.2027, found *m/z* 626.2002. Analytical RP-HPLC (Method IV) t_R = 34.89, 36.34 min.

Diphenyl {1-[2-(3-{[(tert-butoxy)(hydroxy)methyl]amino}-2-oxo-1,2-dihydropyridin-1-yl)propanamido]-2-methylpropyl} phosphonate (13c). Compound **11** (0.12 g, 0.30 mmol), **10c** (84.0 mg, 0.30 mmol), DIPEA (1.30 mL, 0.75 mmol), HBTU (0.14 g, 0.36 mmol) in DMF (2 mL) were reacted and purified as described in the general procedure above to yield a colourless oil **13c** in a diastereomeric mixture (0.12 g, 0.21 mmol, 71%, R_f 0.30, 3:2 in a diastereomeric mixture, Hex:EtOAc). $[\alpha]_{589}^{21}$ = −2.96 (*c* = 0.5, $CHCl_3$). ^{1}H NMR (400 MHz, $CDCl_3$) δ 8.02 (d, *J* = 7.6 Hz, 0.5H), 7.93 (d, *J* = 7.6 Hz, 0.5H), 7.64 (s, 0.5H), 7.57 (s, 0.5H), 7.35−7.00 (m, 11H), 6.88−6.85 (m, 1H), 6.32 (t, *J* = 7.6 Hz, 0.5H), 6.18 (t, *J* = 7.2 Hz, 0.5H), 5.78 (q, *J* = 7.2 Hz, 0.5H), 5.55 (q, *J* = 7.2 Hz, 0.5H), 4.69−4.60 (m, 1H), 2.46−2.29 (m, 1H), 1.64 (d, *J* = 7.2 Hz, 1.5H), 1.55 (d, *J* = 7.2 Hz, 1.5H), 1.51−1.48 (m, 9H), 1.13−1.10 (m, 3H), 0.93−0.91 (m, 1.5H), 0.81−0.79 (m, 1.5H). ^{13}C NMR (101 MHz, $CDCl_3$) δ 169.6 (d, J_{C-P} = 6.6 Hz), 169.5 (d, J_{C-P} = 5.0 Hz), 157.63, 157.61, 152.9, 152.7, 150.6 (d, J_{C-P} = 10.0 Hz), 150.2 (d, J_{C-P} = 9.3 Hz), 150.0 (d, J_{C-P} = 8.9 Hz), 149.9 (d, J_{C-P} = 10.6 Hz), 130.0 (d, J_{C-P} = 1.0 Hz), 129.9 (d, J_{C-P} = 0.8 Hz), 129.8 (d, J_{C-P} = 1.0 Hz), 129.7 (d, J_{C-P} = 1.0 Hz), 125.5 (d, J_{C-P} = 1.2 Hz), 125.38 (d, J_{C-P} = 1.2 Hz), 125.36 (d, J_{C-P} = 1.1 Hz), 124.4, 124.3, 120.8 (d, J_{C-P} = 4.0 Hz), 120.7 (d, J_{C-P} = 4.1 Hz), 120.6 (d, J_{C-P} = 4.5 Hz), 120.5 (d, J_{C-P} = 4.5 Hz), 120.1, 119.9, 107.9, 81.2, 81.0, 53.8, 53.4, 51.5 (d, J_{C-P} = 152.5 Hz), 51.4 (d, J_{C-P} = 155.1 Hz), 29.3 (d, J_{C-P} = 3.5 Hz), 29.2 (d, J_{C-P} = 3.8 Hz), 28.40, 28.39, 20.7 (d, J_{C-P} = 12.8 Hz), 20.4 (d, J_{C-P} = 13.4 Hz), 18.3 (d, J_{C-P} = 5.2 Hz), 17.7 (d, J_{C-P} = 4.4 Hz), 15.3, 15.02. ^{31}P NMR (162 MHz, $CDCl_3$) δ 16.86 (35.6%), 16.30 (64.4%). HRMS-ESI calculated for $C_{29}H_{36}N_3NaO_7P$ [M + Na^+] 592.2183, found *m/z* 592.2187. Analytical RP-HPLC (Method II) t_R = 34.65, 35.90 min.

Phenyl N-[1-({[1-(diphenoxyphosphoryl)-2-methylbutyl]carbamoyl}methyl)-2-oxo-1,2-dihydropyridin-3-yl]carbamate (13d). Compound **12** (73.4 mg, 0.23 mmol), **10a** (69.4 mg, 0.23 mmol), DIPEA (0.10 mL, 0.58 mmol), HBTU (0.10 g, 0.28 mmol) in DMF (2 mL) were reacted and purified as described in the general procedure above to yield a colourless oil **13d** in a diastereomeric mixture (68 mg, 0.11 mmol, 48%, R_f 0.34, 3:2 Hex:EtOAc). $[\alpha]_{589}^{21}$ = −1.75 (*c* = 0.6, $CHCl_3$). ^{1}H NMR (400 MHz, $CDCl_3$) δ 8.07 (br s, 1H), 7.81 (s, 1H), 7.47−7.03 (m, 16H), 6.97−6.93 (m, 1H), 6.29−6.24 (m, 1H), 5.17 (s, 2H), 4.86−4.78 (m, 0.5H), 4.73−4.63 (m, 0.5H), 4.60−4.47 (m, 2H), 2.18−2.09 (m, 0.5H), 1.81−1.75 (m, 0.5H), 1.43−1.32 (m, 1H), 1.27−1.17 (m, 1H), 1.08−1.03 (m, 3H), 0.91−0.86 (m, 3H). ^{13}C NMR (101 MHz, $CDCl_3$) δ 167.0 (d, J_{C-P} = 5.9 Hz), 166.9 (d, J_{C-P} = 6.2 Hz), 157.4, 153.2, 150.19 (d, J_{C-P} = 10.2 Hz), 150.17 (d, J_{C-P} = 10.2 Hz), 150.98 (d, J_{C-P} = 9.3 Hz), 149.97 (d, J_{C-P} = 9.4 Hz), 135.73, 135.71, 129.73 (d, J_{C-P} = 1.0 Hz), 129.70 (d, J_{C-P} = 1.0 Hz), 129.65 (d, J_{C-P} = 0.8 Hz), 129.53, 129.51, 129.4, 129.3, 128.6, 128.4, 128.3, 125.4 (d, J_{C-P} = 1.3 Hz), 125.3 (d, J_{C-P} = 1.1 Hz), 125.2 (d, J_{C-P} = 0.8 Hz), 120.9, 120.60 (d, J_{C-P} = 4.2 Hz), 120.56 (d, J_{C-P} = 4.2 Hz), 120.33 (d, J_{C-P} = 4.3 Hz), 120.31 (d, J_{C-P} = 4.4 Hz), 107.6, 67.2, 54.1, 51.3 (d, J_{C-P} = 154.2 Hz), 49.4 (d, J_{C-P} = 154.4 Hz), 35.9 (d, J_{C-P} = 3.5 Hz), 35.4 (d, J_{C-P} = 3.5 Hz), 27.2 (d, J_{C-P} = 14.9 Hz), 24.8 (d, J_{C-P} = 5.5 Hz), 16.4 (d, J_{C-P} = 11.8 Hz), 15.1 (d, J_{C-P} = 3.2 Hz), 11.6, 11.4. ^{31}P NMR (162 MHz, $CDCl_3$) δ 16.99 (59.3%), 16.55 (40.7%). HRMS-ESI calculated for $C_{32}H_{34}N_3NaO_7P$ [M + Na^+] 626.2027, found *m/z* 626.1982. Analytical RP-HPLC (Method IV) t_R = 34.91, 35.60 min.

Phenyl N-[1-(1-{[1-(diphenoxyphosphoryl)-2-methylbutyl]carbamoyl}ethyl)-2-oxo-1,2-dihydropyridin-3-yl]carbamate (13e). Compound **12** (0.17 g, 0.53 mmol), **10b** (0.15 g, 0.48 mmol), DIPEA (0.20 mL, 1.21 mmol), HBTU (0.22 g, 0.58 mmol) in DMF (2 mL) were reacted and purified as described in the general procedure above to yield a colourless oil **13e** in a diastereomeric mixture (0.17 g, 0.29 mmol, 59%, R_f 0.31, 3:2 Hex:EtOAc). $[\alpha]_{589}^{21}$ = −1.57 (*c* = 0.6, $CHCl_3$). ^{1}H NMR (400 MHz, $CDCl_3$) δ 8.07 (d, *J* = 7.2 Hz, 0.5H), 7.97 (br s, 0.5H), 7.89 (s, 0.5H), 7.80−7.79 (m, 0.5H), 7.46−6.79 (m, 17H), 6.33 (t, *J* = 7.2 Hz, 0.5H), 6.24−6.17 (m, 0.5H), 5.82−5.79 (m, 0.5H), 5.59−5.51 (m, 0.5H), 5.23−5.14 (m, 2H), 4.85−4.76 (m, 0.5H), 4.71−4.61 (m, 0.5H), 2.20−2.14 (m, 0.5H), 1.86−1.78 (m, 0.5H), 1.65−1.63 (m, 1.5H), 1.55−1.52 (m, 1.5H), 1.38−1.25 (m, 2H), 1.15−1.05 (m, 2H), 0.99−0.91 (m, 2H), 0.87−0.81 (m, 1H), 0.79−0.74 (m, 1H). ^{13}C NMR (101 MHz, $CDCl_3$) δ 169.5 (d, J_{C-P} = 6.5 Hz), 169.4 (d, J_{C-P} = 6.5 Hz), 157.48, 157.45, 153.5, 153.2, 150.64 (d, J_{C-P} = 9.7 Hz), 150.56 (d, J_{C-P} = 9.0 Hz), 150.2 (d, J_{C-P} = 9.7 Hz), 150.0 (d, J_{C-P} = 9.1 Hz), 149.9 (d, J_{C-P} = 10.3 Hz), 135.94, 135.92, 129.94 (d, J_{C-P} = 1.1 Hz), 129.93 (d, J_{C-P} = 1.1 Hz), 129.88 (d, J_{C-P} = 0.7 Hz), 129.8 (d, J_{C-P} = 0.9 Hz), 129.7 (d, J_{C-P} = 0.9 Hz), 129.23, 129.21, 129.18, 128.77, 128.75, 128.56, 128.55, 128.53, 128.38, 128.3, 125.53 (d, J_{C-P} = 1.2 Hz), 120.50 (d, J_{C-P} = 1.2 Hz), 125.41 (d, J_{C-P} = 1.0 Hz), 125.35 (d, J_{C-P} = 1.0 Hz), 125.3 (d, J_{C-P} = 1.5 Hz), 125.1, 125.04, 125.02, 120.8 (d, J_{C-P} = 4.3 Hz), 120.73 (d, J_{C-P} = 3.6 Hz), 120.72 (d, J_{C-P} = 4.0 Hz), 120.55 (d, J_{C-P} = 4.0 Hz), 120.47 (d, J_{C-P} = 4.3 Hz), 120.46 (d, J_{C-P} = 4.2 Hz), 120.4, 107.8, 107.73, 107.72, 107.69, 67.4, 67.2, 53.84, 53.76, 53.6, 53.5, 51.4 (d, J_{C-P} = 154.6 Hz), 49.5 (d, J_{C-P} = 152.6 Hz), 49.4 (d, J_{C-P} = 155.9 Hz), 36.00 (d, J_{C-P} = 4.1 Hz), 35.95 (d, J_{C-P} = 3.9 Hz), 35.5 (d, J_{C-P} = 3.9 Hz), 35.4 (d, J_{C-P} = 3.8 Hz), 27.5 (d, J_{C-P} = 14.9 Hz), 27.2 (d, J_{C-P} = 14.9 Hz), 25.2 (d, J_{C-P} = 5.4 Hz), 24.7(d, J_{C-P} = 5.2 Hz), 16.6 (d, J_{C-P} = 10.7 Hz), 16.4 (d, J_{C-P} = 11.3 Hz), 15.5 (d, J_{C-P} = 4.4 Hz), 15.4 (d, J_{C-P} = 3.4 Hz), 15.3, 15.2, 15.0 (d, J_{C-P} = 3.2 Hz), 11.8 (d, J_{C-P} = 1.2 Hz), 11.6 (d, J_{C-P} = 1.2 Hz), 11.5, 11.4. ^{31}P NMR (162 MHz, $CDCl_3$) δ 17.61 (7.2%), 17.12 (5.8%), 16.77 (49.8%), 16.35 (37.1%). HRMS-ESI calculated for $C_{33}H_{36}N_3NaO_7P$ [M + Na^+] 640.2183, found *m/z* 640.2135. Analytical RP-HPLC (Method IV) t_R = 39.11, 39.97, 40.68 min.

Diphenyl {1-[2-(3-{[(tert-butoxy)(hydroxy)methyl]amino}-2-oxo-1,2-dihydropyridin-1-yl)propanamido]-2-methylbutyl}phosphonate (13f). Compound **12** (74.4 mg, 0.23 mmol), **10c** (65.8 mg, 0.23 mmol), DIPEA (150 μL, 0.58 mmol), HBTU (0.11 g, 0.28 mmol) in DMF (2 mL) were reacted and purified as described in the general procedure above to yield a colourless oil **13f** in a diastereomeric mixture (58.0 mg, 0.21 mmol, 43%, R_f 0.33, 3:2 Hex:EtOAc). $[\alpha]_{589}^{21}$ = −1.53 (*c* = 1.0, $CHCl_3$). ^{1}H NMR (400 MHz, $CDCl_3$) δ 8.02 (d, *J* = 7.6 Hz, 0.5H), 7.94 (br s, 0.5H), 7.64 (s, 0.5H), 7.57 (s 0.5H), 7.34−6.98 (m, 11H), 6.91−6.84 (m, 1H), 6.34−6.30 (m, 0.5H), 6.21−6.14 (m, 0.5H), 5.79−5.74 (m, 0.5H), 5.58−5.50 (m, 0.5H), 4.85−4.75 (m, 0.5H), 4.71−4.61 (m, 0.5H), 2.21−2.04 (m, 0.5H), 1.85−1.79 (m, 0.5H), 1.68−1.62 (m, 1.5H), 1.55−1.53 (m, 1.5H), 1.51−1.47 (m, 9H), 1.38−1.26 (m, 1H), 1.14−0.92 (m, 4.5H), 0.89−0.84 (m, 1H), 0.80−0.76 (m, 1.5H). ^{13}C NMR (101 MHz, $CDCl_3$) δ 169.5 (d, J_{C-P} = 6.6 Hz), 169.4 (d, J_{C-P} = 6.5 Hz), 157.63, 157.60, 152.9, 152.7, 150.7 (d, J_{C-P} = 9.8 Hz), 150.6 (d, J_{C-P} = 9.8 Hz), 150.2 (d, J_{C-P} = 9.4 Hz), 150.1 (d, J_{C-P} = 9.0 Hz), 149.9 (d, J_{C-P} = 10.8 Hz), 130.0 (d, J_{C-P} = 1.1 Hz), 129.94 (d, J_{C-P} = 1.1 Hz), 129.89 (d, J_{C-P} = 0.8 Hz), 129.76 (d, J_{C-P} = 1.6 Hz), 129.75 (d, J_{C-P} = 1.7 Hz), 129.72 (d, J_{C-P} = 1.0 Hz), 125.54 (d, J_{C-P} = 1.3 Hz), 125.50 (d, J_{C-P} = 1.2 Hz), 125.38, 125.35, 125.33, 124.42, 124.36, 124.3, 120.8 (d, J_{C-P} = 4.0 Hz), 120.74 (d, J_{C-P} = 4.4 Hz), 120.72 (d, J_{C-P} = 4.0 Hz), 120.6 (d, J_{C-P} = 4.6 Hz), 120.50 (d, J_{C-P} = 4.4 Hz), 120.46 (d, J_{C-P} = 4.5 Hz), 120.1, 119.9, 107.9, 81.2, 81.0, 53.82, 53.76, 53.41, 53.35, 51.4 (d, J_{C-P} = 153.0 Hz), 49.5 (d, J_{C-P} = 153.0 Hz), 49.3 (d, J_{C-P} = 155.7 Hz), 36.0 (d, J_{C-P} = 4.2 Hz), 36.0 (d, J_{C-P} = 4.2 Hz), 35.5 (d, J_{C-P} = 3.5 Hz), 35.4 (d, J_{C-P} = 3.8 Hz), 28.4, 27.5 (d, J_{C-P} = 14.9 Hz), 27.2 (d, J_{C-P} = 15.0 Hz), 25.2 (d, J_{C-P} = 5.7 Hz), 24.7 (d, J_{C-P} = 5.4 Hz), 16.6 (d, J_{C-P} = 6.6 Hz), 16.4 (d, J_{C-P} = 10.6 Hz), 16.4 (d, J_{C-P} = 11.3 Hz), 15.34 (d, J_{C-P} = 5.5 Hz), 15.4 (d, J_{C-P} = 3.6 Hz), 15.3 (d, J_{C-P} = 5.6 Hz), 15.14, 15.13, 15.0 (d, J_{C-P} = 3.2 Hz), 11.8 (d, J_{C-P} = 1.2 Hz), 11.7 (d, J_{C-P} = 1.0 Hz), 11.5, 11.4. ^{31}P NMR (162 MHz, $CDCl_3$) δ 17.44 (14.5%), 16.93 (12.3%), 16.82 (40.2%), 16.37 (33.0%). HRMS-ESI calculated for $C_{30}H_{38}N_3NaO_7P$ [M + Na^+] 606.2340, found *m/z* 606.2359. Analytical RP-HPLC (Method IV) t_R = 39.18, 40.00, 40.67 min.

Benzyl N-{1-[(1S)-{[1-(diphenoxyphosphoryl)-2-methylpropyl]carbamoyl}ethyl]-2-oxo-1,2-dihydropyridin-3-yl}

carbamate (18a). Compound **11** (0.15 g, 0.38 mmol), **17** (0.10 g, 0.32 mmol), DIPEA (140 μL, 0.79 mmol), HBTU (0.14 g, 0.38 mmol) in DMF (4 mL) were reacted and purified as described in the general procedure above to yield a colourless oil **18a** (47 mg, 0.078 mmol, 25%, R_f = 0.23 in 7:3 PE:EtOAc). $[\alpha]_{589}^{21}$ = −1.10 (*c* = 0.6, $CHCl_3$). ^{1}H NMR (400 MHz, $CDCl_3$) δ 7.98 (d, *J* = 7.2 Hz, 0.5H), 7.88 (d, *J* = 7.6 Hz, 0.5H), 7.81 (s, 0.5H), 7.71 (s, 0.5H), 7.40–6.76 (m, 17H), 6.24 (t, *J* = 7.2 Hz, 0.5H), 6.11 (t, *J* = 7.2 Hz, 0.5H), 5.72 (q, *J* = 7.2 Hz, 0.5H), 5.47 (q, *J* = 7.2 Hz, 0.5H), 5.10 (s, 1H), 5.04 (s, 1H), 4.67–4.49 (m, 1H), 2.35–2.19 (m, 1H), 1.55 (d, *J* = 7.2 Hz, 1.5H), 1.44 (d, *J* = 7.2 Hz, 1.5H), 1.04–1.00 (m, 3H), 0.82 (d, *J* = 6.8 Hz, 1.5H), 0.72–0.69 (m, 1.5H). ^{13}C NMR (101 MHz, $CDCl_3$) δ 169.6 (d, $J_{C\text{-}P}$ = 6.6 Hz), 157.5, 157.4, 153.5, 153.3, 150.6 (d, $J_{C\text{-}P}$ = 9.8 Hz), 150.2 (d, $J_{C\text{-}P}$ = 9.2 Hz), 150.0 (d, $J_{C\text{-}P}$ = 9.3 Hz), 149.9 (d, $J_{C\text{-}P}$ = 10.5 Hz), 136.0, 135.9, 129.94 (d, $J_{C\text{-}P}$ = 0.9 Hz), 129.89 (d, $J_{C\text{-}P}$ = 0.7 Hz), 129.8 (d, $J_{C\text{-}P}$ = 1.0 Hz), 129.7 (d, $J_{C\text{-}P}$ = 0.9 Hz), 129.22, 129.18, 128.81, 128.77, 128.74, 128.64, 128.61, 128.56, 128.52, 128.38, 128.37, 125.5 (d, $J_{C\text{-}P}$ = 1.1 Hz), 125.40 (d, $J_{C\text{-}P}$ = 1.3 Hz), 125.38 (d, $J_{C\text{-}P}$ = 0.9 Hz), 125.3 (d, $J_{C\text{-}P}$ = 1.2 Hz), 125.1, 120.8 (d, $J_{C\text{-}P}$ = 4.3 Hz), 120.7 (d, $J_{C\text{-}P}$ = 4.2 Hz), 120.58, 120.6, 120.46 (d, $J_{C\text{-}P}$ = 4.2 Hz), 120.45 (d, $J_{C\text{-}P}$ = 4.4 Hz), 107.7, 67.4, 67.2, 53.8, 53.6, 51.6 (d, $J_{C\text{-}P}$ = 152.7 Hz), 51.5 (d, $J_{C\text{-}P}$ = 154.9 Hz), 29.23 (d, $J_{C\text{-}P}$ = 3.6 Hz), 29.17 (d, $J_{C\text{-}P}$ = 3.7 Hz), 20.7 (d, $J_{C\text{-}P}$ = 11.9 Hz), 20.4 (d, $J_{C\text{-}P}$ = 12.3 Hz), 18.4 (d, $J_{C\text{-}P}$ = 5.2 Hz), 17.7 (d, $J_{C\text{-}P}$ = 4.9 Hz), 15.6, 15.3. ^{31}P NMR (162 MHz, $CDCl_3$) δ 17.06 (17.4%), 16.28 (82.6%). HRMS-ESI calculated for $C_{32}H_{35}N_3O_7P$ [M + H^+] 604.2207, found *m/z* 604.2189. Analytical RP-HPLC (Method IV) t_R = 34.70, 36.14 min.

Benzyl N-{1-[(1S)-1-{[1-(diphenoxyphosphoryl)-2-methylbutyl]carbamoyl}ethyl]-2-oxo-1,2-dihydropyridin-3-yl} carbamate (18b). Compound **12** (39.6 mg, 0.12 mmol), **17** (32.6 mg, 0.10 mmol), DIPEA (45 μL, 0.26 mmol), HBTU (47.0 mg, 0.12 mmol) in DMF (2 mL) were reacted and purified as described in the general procedure above to yield a colourless oil **18b** (27 mg, 0.044 mmol, 42%, R_f = 0.26 in 7:3 PE:EtOAc). $[\alpha]_{589}^{21}$ = −0.20 (*c* = 0.6, $CHCl_3$). ^{1}H NMR (400 MHz, $CDCl_3$) δ 8.07 (d, *J* = 7.2 Hz, 0.5H), 7.97 (br s, 0.5H), 7.89 (s, 0.5H), 7.81–7.79 (m, 0.5H), 7.41–6.87 (m, 17H), 6.33 (t, *J* = 7.2 Hz, 0.5H), 6.24–6.17 (m, 0.5H), 5.82–5.79 (m, 0.5H), 5.59–5.51 (m, 0.5H), 5.23–5.14 (m, 2H), 4.85–4.76 (m, 0.5H), 4.71–4.61 (m, 0.5H), 2.20–2.04 (m, 0.5H), 1.88–1.78 (m, 0.5H), 1.68–1.60 (m, 1.5H), 1.54–1.50 (m, 1.5H), 1.39–1.25 (m, 2H), 1.15–1.05 (m, 2H), 0.97–0.91 (m, 2H), 0.88–0.82 (m, 1H), 0.80–0.75 (m, 1H). ^{13}C NMR (101 MHz, $CDCl_3$) δ 169.5 (d, $J_{C\text{-}P}$ = 6.3 Hz), 169.4 (d, $J_{C\text{-}P}$ = 6.3 Hz), 157.47, 157.43, 153.5, 153.2, 150.63 (d, $J_{C\text{-}P}$ = 9.9 Hz), 150.57 (d, $J_{C\text{-}P}$ = 9.8 Hz), 150.2 (d, $J_{C\text{-}P}$ = 9.7 Hz), 150.0 (d, $J_{C\text{-}P}$ = 9.0 Hz), 149.9 (d, $J_{C\text{-}P}$ = 10.6 Hz), 135.94, 135.91, 129.94 (d, $J_{C\text{-}P}$ = 1.1 Hz), 129.93 (d, $J_{C\text{-}P}$ = 1.1 Hz), 129.88 (d, $J_{C\text{-}P}$ = 0.7 Hz), 129.77 (d, $J_{C\text{-}P}$ = 1.0 Hz), 129.73 (d, $J_{C\text{-}P}$ = 1.0 Hz), 129.70 (d, $J_{C\text{-}P}$ = 0.8 Hz), 129.22, 129.21, 129.19, 129.16, 128.8, 128.7, 128.6, 128.54, 128.52, 128.4, 128.3, 125.53 (d, $J_{C\text{-}P}$ = 1.2 Hz), 120.50 (d, $J_{C\text{-}P}$ = 1.2 Hz), 125.41 (d, $J_{C\text{-}P}$ = 1.0 Hz), 125.35 (d, $J_{C\text{-}P}$ = 1.0 Hz), 125.3 (d, $J_{C\text{-}P}$ = 1.6 Hz), 125.14, 125.08, 125.04, 120.8 (d, $J_{C\text{-}P}$ = 4.2 Hz), 120.72 (d, $J_{C\text{-}P}$ = 3.9 Hz), 120.70 (d, $J_{C\text{-}P}$ = 4.0 Hz), 120.57, 120.55, 120.48 (d, $J_{C\text{-}P}$ = 4.3 Hz), 120.46 (d, $J_{C\text{-}P}$ = 4.4 Hz), 120.45 (d, $J_{C\text{-}P}$ = 4.4 Hz), 120.4, 107.71, 107.68, 67.4, 67.2, 53.83, 53.76, 53.6, 53.5, 51.4 (d, $J_{C\text{-}P}$ = 154.0 Hz), 49.5 (d, $J_{C\text{-}P}$ = 153.1 Hz), 49.4 (d, $J_{C\text{-}P}$ = 156.6 Hz), 36.0 (d, $J_{C\text{-}P}$ = 4.2 Hz), 35.9 (d, $J_{C\text{-}P}$ = 3.8 Hz), 35.5 (d, $J_{C\text{-}P}$ = 3.6 Hz), 35.4 (d, $J_{C\text{-}P}$ = 3.8 Hz), 27.4 (d, $J_{C\text{-}P}$ = 14.5 Hz), 27.2 (d, $J_{C\text{-}P}$ = 14.9 Hz), 25.2 (d, $J_{C\text{-}P}$ = 5.9 Hz), 24.7 (d, $J_{C\text{-}P}$ = 5.3 Hz), 16.6 (d, $J_{C\text{-}P}$ = 10.3 Hz), 16.4 (d, $J_{C\text{-}P}$ = 11.7 Hz), 15.6 (d, $J_{C\text{-}P}$ = 5.8 Hz), 15.4 (d, $J_{C\text{-}P}$ = 3.1 Hz), 15.34, 15.25, 15.0 (d, $J_{C\text{-}P}$ = 1.1 Hz), 11.8 (d, $J_{C\text{-}P}$ = 1.0 Hz), 11.6, 11.5, 11.4. ^{31}P NMR (162 MHz, $CDCl_3$) δ 17.60 (9.3%), 17.16 (7.3%), 16.78 (52.9%), 16.37 (30.5%). HRMS-ESI calculated for $C_{33}H_{36}N_3NaO_7P$ [M + Na^+] 640.2183, found *m/z* 640.2164. Analytical RP-HPLC (Method IV) t_R = 38.92, 39.76, 40.44, min.

Diphenyl (1-{[(2S)-1-[(2S)-2-(2,2-dimethylpropanamido)-3,3-dimethylbutanoyl]pyrrolidin-2-yl]formamido}-2-methylpropyl) phosphonate (28a). Compound **12** (0.12 g, 0.38 mmol), **27c** (78 mg, 0.25 mmol), DIPEA (0.10 mL, 0.63 mmol), HBTU (0.11 g, 0.30 mmol) in DMF (2 mL) were reacted and purified as described in the general procedure above to yield a colourless oil **28a** (0.13 mg, 0.21 mmol, 82%, R_f 0.33, 0.21 in 1:1 Hex:EtOAc). $[\alpha]_{589}^{21}$ = −73.40 (*c* = 0.5, CH_3OH). ^{1}H NMR (400 MHz, CD_3OD) δ 7.40–7.09 (m, 10H), 6.78–6.75 (m, 1H), 4.96–4.88 (m, 1H), 4.72–4.63 (m, 2.5H), 4.54–4.48 (m, 0.5H), 3.94–3.84 (m, 1H), 3.78–3.68 (m, 1H), 2.31–2.25 (m, 0.5H), 2.17–2.05 (m, 2H), 2.03–1.92 (m, 1H), 1.90–1.73 (m, 1.5H), 1.49–1.41 (m, 1H), 1.38–1.28 (m, 1H), 1.28–1.17 (m, 11H), 1.12–1.09 (m, 1H), 1.03–0.98 (m, 9H), 0.96–0.92 (m, 3H). ^{13}C NMR (101 MHz, CD_3CN) δ 178.31, 178.30, 173.1 (d, $J_{C\text{-}P}$ = 5.5 Hz), 172.88 (d, $J_{C\text{-}P}$ = 5.7 Hz), 172.85 (d, $J_{C\text{-}P}$ = 5.9 Hz), 171.83, 171.80, 151.4 (d, $J_{C\text{-}P}$ = 10.1 Hz), 151.22 (d, $J_{C\text{-}P}$ = 8.4 Hz), 151.21 (d, $J_{C\text{-}P}$ = 8.9 Hz), 151.17 (d, $J_{C\text{-}P}$ = 10.3 Hz), 151.15 (d, $J_{C\text{-}P}$ = 10.4 Hz), 130.9 (d, $J_{C\text{-}P}$ = 1.2 Hz), 130.83 (d, $J_{C\text{-}P}$ = 1.2 Hz), 130.75 (d, $J_{C\text{-}P}$ = 1.1 Hz), 130.7 (d, $J_{C\text{-}P}$ = 1.0 Hz), 126.38 (d, $J_{C\text{-}P}$ = 1.4 Hz), 126.36 (d, $J_{C\text{-}P}$ = 1.5 Hz), 126.33 (d, $J_{C\text{-}P}$ = 1.1 Hz), 126.28 (d, $J_{C\text{-}P}$ = 1.4 Hz), 122.1 (d, $J_{C\text{-}P}$ = 3.9 Hz), 121.8 (d, $J_{C\text{-}P}$ = 4.2 Hz), 121.7 (d, $J_{C\text{-}P}$ = 4.0 Hz), 121.5 (d, $J_{C\text{-}P}$ = 4.4 Hz), 61.21, 61.18, 60.91, 60.87, 57.4, 51.7 (d, $J_{C\text{-}P}$ = 153.4 Hz), 51.2 (d, $J_{C\text{-}P}$ = 153.2 Hz), 49.4, 48.9 (d, $J_{C\text{-}P}$ = 154.1 Hz), 39.4, 37.1 (d, $J_{C\text{-}P}$ = 4.6 Hz), 36.9 (d, $J_{C\text{-}P}$ = 4.4 Hz), 36.7 (d, $J_{C\text{-}P}$ = 4.4 Hz), 36.4 (d, $J_{C\text{-}P}$ = 4.0 Hz), 30.2, 30.1, 29.5, 29.4, 28.0 (d, $J_{C\text{-}P}$ = 15.0 Hz), 27.77, 27.76, 27.6 (d, $J_{C\text{-}P}$ = 15.3 Hz), 26.8, 26.7, 25.94, 25.87, 25.73, 25.66, 16.9 (d, $J_{C\text{-}P}$ = 11.5 Hz), 16.7 (d, $J_{C\text{-}P}$ = 10.9 Hz), 16.0 (d, $J_{C\text{-}P}$ = 3.4 Hz), 15.8 (d, $J_{C\text{-}P}$ = 2.8 Hz), 12.03, 12.02, 11.7, 11.6. ^{31}P NMR (162 MHz, CD_3OD) δ 18.76 (26.3%), 18.32 (10.3%), 18.24 (32.2%), 17.99 (31.2%). HRMS-ESI calculated for $C_{33}H_{48}N_3NaO_6P$ [M + Na^+] 636.3173, found *m/z* 636.3159. Analytical RP-HPLC (Method III) t_R = 40.17, 40.95, 41.22, 43.03 min.

Diphenyl (1-{[(2S)-1-[(2S)-2-[(tert-butylcarbamoyl)amino]-3,3-dimethylbutanoyl]pyrrolidin-2-yl]formamido}-2-methylpropyl)phosphonate (28b). Compound **11** (46.1 mg, 0.15 mmol), **27b** (49.3 mg, 0.15 mmol), DIPEA (65 μL, 0.38 mmol), HBTU (68.6 mg, 0.18 mmol) in DMF (2 mL) were reacted and purified as described in the general procedure above to yield a colourless oil **28b** (53.3 mg, 0.087 mmol, 57%, R_f 0.21 in 1:1 Hex:EtOAc). $[\alpha]_{589}^{21}$ = −57.60 (*c* = 0.5, $CHCl_3$). ^{1}H NMR (400 MHz, $CDCl_3$) δ 8.00 (s, 0.5H), 7.89 (d, *J* = 10.4, 0.5H), 7.35 (d, *J* = 10.4, 0.5H), 7.30–7.07 (m, 10H), 6.86–6.82 (m, 0.5H), 5.63 (bd, *J* = 9.6 Hz, 0.5H), 5.14 (d, *J* = 9.6 Hz, 0.5H), 4.83–4.67 (m, 2H), 4.58 (d, *J* = 9.6 Hz, 0.5H), 4.49 (d, *J* = 9.2 Hz, 0.5H), 3.93–3.84 (m, 1H), 3.74–3.69 (m, 0.5H), 3.62–3.57 (m, 0.5H), 2.45–2.38 (m, 0.5H), 2.36–2.30 (m, 0.5H), 2.21 (br, 0.5H), 2.10–2.03 (m, 0.5H), 1.95–1.78 (m, 3H), 1.29–1.24 (m, 9H), 1.11–1.04 (m, 6H), 0.97–0.93 (m, 9H). ^{13}C NMR (101 MHz, $CDCl_3$) δ 173.8, 172.9 (d, $J_{C\text{-}P}$ = 8.1 Hz), 172.8, 172.1 (d, $J_{C\text{-}P}$ = 6.1 Hz), 157.4, 157.1, 150.5 (d, $J_{C\text{-}P}$ = 10.1 Hz), 150.4 (d, $J_{C\text{-}P}$ = 10.1 Hz), 150.2 (d, $J_{C\text{-}P}$ = 10.1 Hz), 150.1 (d, $J_{C\text{-}P}$ = 10.1 Hz), 129.91, 129.89 (d, $J_{C\text{-}P}$ = 0.8 Hz), 129.84 (d, $J_{C\text{-}P}$ = 0.7 Hz), 125.48 (d, $J_{C\text{-}P}$ = 1.1 Hz), 125.46 (d, $J_{C\text{-}P}$ = 0.9 Hz), 125.34 (d, $J_{C\text{-}P}$ = 0.7 Hz), 125.29 (d, $J_{C\text{-}P}$ = 0.8 Hz), 120.9 (d, $J_{C\text{-}P}$ = 4.0 Hz), 120.8 (d, $J_{C\text{-}P}$ = 4.1 Hz), 120.55 (d, $J_{C\text{-}P}$ = 4.1 Hz), 120.48 (d, $J_{C\text{-}P}$ = 4.4 Hz), 60.5, 59.8, 57.5, 57.3, 51.3 (d, $J_{C\text{-}P}$ = 155.6 Hz) 51.1 (d, $J_{C\text{-}P}$ = 153.6 Hz), 50.4, 50.2, 48.9, 48.8, 36.1, 35.4, 29.73, 29.67, 29.6, 29.44 (d, J_{C-P} = 4.6 Hz), 29.40 (d, J_{C-P} = 4.3 Hz), 29.0, 28.3, 26.6, 26.5, 25.4, 25.2, 20.7 (d, $J_{C\text{-}P}$ = 13.1 Hz), 20.4 (d, J_{C-P} = 13.2 Hz), 18.4 (d, J_{C-P} = 5.9 Hz), 18.2 (d, J_{C-P} = 4.9 Hz). ^{31}P NMR (162 MHz, $CDCl_3$) δ 17.90 (52.7%), 17.04 (47.3%). HRMS-ESI calculated for $C_{32}H_{47}N_4NaO_6P$ [M + Na^+] 637.3125, found *m/z* 637.3121. Analytical RP-HPLC (Method I) t_R = 27.22, 27.36 min.

Diphenyl (1-{[(2S)-1-[(2S)-2-[(tert-butylcarbamoyl)amino]-3,3-dimethylbutanoyl]pyrrolidin-2-yl]formamido}-2-methylbutyl)phosphonate (28c). Compound **12** (49.4 mg, 0.15 mmol), **27b** (50.0 mg, 0.15 mmol), DIPEA (66 μL, 0.38 mmol), HBTU (69.6 mg, 0.18 mmol) in DMF (2 mL) were reacted and

purified as described in the general procedure above to yield a colourless oil **28c** (76 mg, 0.095 mmol, 62%, R_f 0.21 in 1:1 Hex:EtOAc). $[\alpha]_{589}^{21} = -67.00$ ($c = 0.5$, $CHCl_3$). ^{1}H NMR (400 MHz, $CDCl_3$) δ 7.86–7.79 (m, 1H), 7.40–7.09 (m, 11H), 5.57 (d, J = 9.6, 1H), 5.04–4.96 (m, 0.5H), 4.89–4.81 (m, 0.5H), 4.74–4.70 (m, 1H), 4.58 (d, J = 10 Hz, 0.5H), 4.50–4.47 (m, 0.5H), 3.92–3.81 (m, 1H), 3.73–3.69 (m, 0.5H), 3.60–3.56 (m, 0.5H), 2.28 (br, 0.5H), 2.10–2.04 (m, 1.5H), 1.91–1.71 (m, 4H), 1.54–1.39 (m, 1H), 1.29–1.24 (m, 9H), 1.15–1.03 (m, 3H), 0.97–0.77 (m, 12H). ^{13}C NMR (101 MHz, $CDCl_3$) δ 174.0, 173.9, 172.81, 172.78, 172.7 (d, $J_{C\text{-}P}$ = 4.7 Hz), 172.6 (d, $J_{C\text{-}P}$ = 6.4 Hz), 171.8 (d, $J_{C\text{-}P}$ = 5.4 Hz), 171.7 (d, $J_{C\text{-}P}$ = 4.9 Hz), 157.31, 157.29, 156.99, 156.98, 150.5 (d, $J_{C\text{-}P}$ = 10.3 Hz), 150.4 (d, $J_{C\text{-}P}$ = 9.8 Hz), 150.2 (d, $J_{C\text{-}P}$ = 8.8 Hz), 150.1 (d, $J_{C\text{-}P}$ = 10.0 Hz), 129.91 (d, $J_{C\text{-}P}$ = 1.7 Hz), 129.87 (d, $J_{C\text{-}P}$ = 1.6 Hz), 129.80, 129.78, 125.42 (d, $J_{C\text{-}P}$ = 2.3 Hz), 125.37, 125.34, 125.26, 121.0 (d, $J_{C\text{-}P}$ = 4.3 Hz), 120.91 (d, $J_{C\text{-}P}$ = 2.4 Hz), 120.87 (d, $J_{C\text{-}P}$ = 1.4 Hz), 120.8, 120.54 (d, $J_{C\text{-}P}$ = 2.8 Hz), 120.51, 120.47 (d, $J_{C\text{-}P}$ = 2.4 Hz), 60.5, 59.7, 59.6, 57.4, 57.3, 51.07 (d, $J_{C\text{-}P}$ = 153.8 Hz), 51.05 (d, $J_{C\text{-}P}$ = 154.9 Hz), 50.5, 50.2, 49.1 (d, $J_{C\text{-}P}$ = 155.0 Hz), 49.0 (d, $J_{C\text{-}P}$ = 156.1 Hz), 48.9, 48.8, 36.3 (d, $J_{C\text{-}P}$ = 4.1 Hz), 36.1, 35.9 (d, $J_{C\text{-}P}$ = 4.1 Hz), 35.7 (d, $J_{C\text{-}P}$ = 3.5 Hz), 35.3 (d, $J_{C\text{-}P}$ = 3.6 Hz), 29.74, 29.66, 29.6, 28.92, 28.85, 28.0, 27.9, 27.5 (d, $J_{C\text{-}P}$ = 15.1 Hz), 26.9 (d, $J_{C\text{-}P}$ = 14.5 Hz), 26.61, 26.6, 26.5, 25.4, 25.3, 25.1, 25.0, 16.6 (d, $J_{C\text{-}P}$ = 11.8 Hz), 16.1 (d, $J_{C\text{-}P}$ = 12.3 Hz), 15.8 (d, $J_{C\text{-}P}$ = 3.8 Hz), 15.3 (d, $J_{C\text{-}P}$ = 3.0 Hz), 11.92, 11.86, 11.7, 11.3. ^{31}P NMR (162 MHz, $CDCl_3$) δ 18.17 (24.5%), 17.80 (14.6%), 17.55 (34.1%), 17.25 (26.8%). HRMS-ESI calculated for $C_{33}H_{49}N_4NaO_6P$ [M + Na^+] 651.3282, found *m/z* 651.3269. Analytical RP-HPLC (Method I) t_R = 30.00, 30.42, 30.78 min.

(Benzyloxy)carbonyl-N-[(2S)-1-[(2S)-2-{[1-(diphenoxyphosphoryl)-2-methylpropyl]carbamoyl}pyrrolidin-1-yl]-2,2-dimethyl-1-oxobutan-2-yl]carbamate (28d). Compound **11** (0.13 g, 0.34 mmol), **27a** (0.12 g, 0.34 mmol), DIPEA (150 μL, 0.85 mmol), HBTU (0.15 g, 0.41 mmol) in DMF (2 mL) were reacted and purified as described in the general procedure above to yield a colourless oil **28d** (0.14 g, 0.22 mmol, 65%, R_f 0.52 in 1:1 Hex:EtOAc). $[\alpha]_{589}^{21} = -58.60$ (c = 0.5, $CHCl_3$). ^{1}H NMR (400 MHz, $CDCl_3$) 7.34–7.12 (m, 16H), 5.73 (d, J = 9.6, 0.5H), 5.53 (d, J = 9.6, 0.5H), 5.12–5.02 (m, 2H), 4.79–4.70 (m, 1.5H), 4.52–4.49 (m, 0.5H), 4.40–4.34 (m, 1H), 3.82–3.77 (m, 1H), 3.68–3.64 (m, 0.5H), 3.61–3.57 (m, 0.5H), 2.47–2.33 (m, 1H), 2.15–1.83 (m, 4H), 1.26–1.02 (m, 6H), 0.98–0.92 (m, 9H). ^{13}C NMR (101 MHz, $CDCl_3$) δ 172.5, 171.8 (d, $J_{C\text{-}P}$ = 6.9 Hz), 171.7, 171.6 (d, $J_{C\text{-}P}$ = 5.5 Hz), 156.6, 156.5, 150.6 (d, $J_{C\text{-}P}$ = 10.1 Hz), 150.3 (d, $J_{C\text{-}P}$ = 10.1 Hz), 150.1, 136.4, 136.3, 129.91 (d, $J_{C\text{-}P}$ = 0.9 Hz), 129.87 (d, $J_{C\text{-}P}$ = 0.8 Hz), 129.83 (d, $J_{C\text{-}P}$ = 0.6 Hz) 129.77 (d, $J_{C\text{-}P}$ = 0.8 Hz), 128.7, 128.32, 128.29, 128.21, 128.19, 125.43 (d, $J_{C\text{-}P}$ = 1.4 Hz), 125.41 (d, $J_{C\text{-}P}$ = 1.5 Hz), 125.3 (d, $J_{C\text{-}P}$ = 0.8 Hz), 125.2 (d, $J_{C\text{-}P}$ = 0.9 Hz), 121.0 (d, $J_{C\text{-}P}$ = 4.0 Hz), 120.80 (d, $J_{C\text{-}P}$ = 1.7 Hz), 120.75 (d, $J_{C\text{-}P}$ = 1.3 Hz), 120.5 (d, $J_{C\text{-}P}$ = 4.4 Hz), 67.2, 67.1, 60.6, 60.3, 59.2, 51.4 (d, $J_{C\text{-}P}$ = 154.7 Hz), 51.2 (d, $J_{C\text{-}P}$ = 154.7 Hz), 48.82, 48.79, 35.8, 35.4, 29.5 (d, $J_{C\text{-}P}$ = 4.1 Hz), 29.4 (d, $J_{C\text{-}P}$ = 3.9 Hz), 28.1, 27.9, 26.4, 26.3, 25.5, 25.2, 20.7 (d, $J_{C\text{-}P}$ = 13.7 Hz), 20.4 (d, $J_{C\text{-}P}$ = 13.4 Hz), 18.2 (d, $J_{C\text{-}P}$ = 4.6 Hz), 18.1 (d, $J_{C\text{-}P}$ = 4.6 Hz). ^{31}P NMR (162 MHz, $CDCl_3$) δ 17.59 (24.7%), 16.92 (75.3%). HRMS-ESI calculated for $C_{35}H_{44}N_3NaO_7P$ [M + Na^+] 672.2809, found *m/z* 672.2783. Analytical RP-HPLC (Method II) t_R = 45.94, 46.32 min.

(Benzyloxy)carbonyl-N-[(2S)-1-[(2S)-2-{[1-(diphenoxyphosphoryl)-2-methylbutyl]carbamoyl}pyrrolidin-1-yl]-3,3-dimethyl-1-oxobutan-2-yl]carbamate (28e). Compound **12** (0.15 g, 0.47 mmol), **27a** (0.15 g, 0.43 mmol), DIPEA (0.20 mL, 1.06 mmol), HBTU (0.19 g, 0.51 mmol) in DMF (2 mL) were reacted and purified as described in the general procedure above to yield a colourless oil **28e** (0.15 g, 0.23 mmol, 55%, R_f 0.47, 0.41 in 1:1 Hex:EtOAc). $[\alpha]_{589}^{21} = -58.10$ (c = 1.0, $CHCl_3$). ^{1}H NMR (400 MHz, $CDCl_3$) δ 7.34–7.12 (m, 16H), 5.65 (d, J = 9.6 Hz, 0.5H), 5.58–5.52 (br s, 0.5H), 5.13–5.02 (m, 2H), 4.96–4.88 (m, 0.5H), 4.82–4.72 (m, 0.5H), 4.47–4.45 (m, 1H), 4.39–4.33 (m, 1H), 3.80–3.77 (m, 1H), 3.68–3.66 (m, 0.5H), 3.62–3.56 (m, 0.5H), 2.36 (br, 0.5H), 2.18–2.04 (m, 2H), 1.98–1.91 (m, 1.5H), 1.86–1.76 (m, 1H), 1.51–1.42 (m, 1H), 1.34–1.23 (m, 1H), 1.18–1.04 (m, 3H), 1.03–0.83 (m, 12H). ^{13}C NMR (101 MHz, $CDCl_3$) δ 171.7 (d, $J_{C\text{-}P}$ = 5.1 Hz), 171.6, 171.4 (d, $J_{C\text{-}P}$ = 6.3 Hz), 156.54, 156.53, 150.6 (d, $J_{C\text{-}P}$ = 10.1 Hz), 150.3 (d, $J_{C\text{-}P}$ = 9.1 Hz), 150.26 (d, $J_{C\text{-}P}$ = 10.6 Hz), 136.38, 136.37, 129.92 (d, $J_{C\text{-}P}$ = 1.0 Hz), 129.89 (d, $J_{C\text{-}P}$ = 0.9 Hz), 129.88 (d, $J_{C\text{-}P}$ = 1.1 Hz), 129.82, 129.77 (d, $J_{C\text{-}P}$ = 0.7 Hz), 129.75 (d, $J_{C\text{-}P}$ = 0.8 Hz), 128.7, 128.3, 128.22, 128.19, 125.43 (d, $J_{C\text{-}P}$ = 0.9 Hz), 125.39 (d, $J_{C\text{-}P}$ = 1.2 Hz), 125.3 (d, $J_{C\text{-}P}$ = 1.3 Hz), 125.2 (d, $J_{C\text{-}P}$ = 0.8 Hz), 120.9 (d, $J_{C\text{-}P}$ = 4.2 Hz), 120.85 (d, $J_{C\text{-}P}$ = 4.8 Hz), 120.82, 120.81, 120.80, 120.78, 120.77, 120.74, 120.52 (d, $J_{C\text{-}P}$ = 4.4 Hz), 120.50 (d, $J_{C\text{-}P}$ = 4.4 Hz), 67.1, 60.5, 60.3, 59.2, 51.3 (d, $J_{C\text{-}P}$ = 153.2 Hz), 51.1 (d, $J_{C\text{-}P}$ = 154.5 Hz), 49.4 (d, $J_{C\text{-}P}$ = 155.2 Hz), 49.2 (d, $J_{C\text{-}P}$ = 155.2 Hz), 48.9, 48.8, 48.6, 48.4, 36.33 (d, $J_{C\text{-}P}$ = 3.8 Hz), 36.28 (d, $J_{C\text{-}P}$ = 5.0 Hz), 35.8 (d, $J_{C\text{-}P}$ = 5.4 Hz), 35.7 (d, $J_{C\text{-}P}$ = 3.7 Hz), 35.4, 28.1, 27.9, 27.5 (d, $J_{C\text{-}P}$ = 14.9 Hz), 27.0 (d, $J_{C\text{-}P}$ = 14.9 Hz), 26.34, 26.31, 25.5, 25.2, 25.0 (d, $J_{C\text{-}P}$ = 4.6 Hz), 24.9 (d, $J_{C\text{-}P}$ = 5.5 Hz), 16.6 (d, $J_{C\text{-}P}$ = 12.1 Hz), 16.3 (d, $J_{C\text{-}P}$ = 12.1 Hz), 15.3 (d, $J_{C\text{-}P}$ = 2.7 Hz), 11.9, 11.8, 11.7, 11.5. ^{31}P NMR (162 MHz, $CDCl_3$) δ 17.96 (8.8%), 17.66 (5.1%), 17.38 (52.3%), 16.99 (33.8%). HRMS-ESI calculated for $C_{36}H_{46}N_3NaO_7P$ [M + Na^+] 686.2966, found *m/z* 686.2944. Analytical RP-HPLC (Method II). t_R = 50.99, 51.22, 51.72, 52.41 min.

4.2. Biological assays

4.2.1. CtHtrA and HNE enzyme assays

CtHtrA recombinant protein purification and assay protocols have been established as previously outlined [54,55]. Assays were performed in 96-well black assay plates, where 2.5 μM of CtHtrA per well was treated against a six-dose series of **JO146** (0.01–125 μM) and equal volumes of DMSO. CtHtrA and inhibitors were diluted to an equal total volume in 50 mM Tris, 20 mM $MgCl_2$ at pH 7.0. Plates were warmed at 37 °C for 10 min to allow for CtHtrA activation prior to addition of 10 μL substrate (prepared in 1 mg/mL in a mixture of 1:1 isopropanol:buffer). MeOCoum-ENLHLPLPIIF-DNP (Mimotopes) was used as the substrate, where MeOCoum represents an N-terminal 7-methoxycoumarin-4-acetic acid fluorophore and DNP represents a C-terminal 2,4-dinitrophenyl-lysine quencher. Proteolysis was then monitored over 30 min at 37 °C using an Infinite M200 Plate Reader (Tecan, Switzerland), taking readings every 30 s with 10 × flashes per well at 340 nm excitation, 405 nm emission. Plates were orbitally shaken for 1 s prior to each reading with 1 mm amplitude, and multiple reads (3 × 3) were taken from each well; gain was calculated based on DMSO control wells. All compounds were tested in triplicate at each dose, alongside an n = 3 dose series of **JO146** and n = 6 DMSO controls. Data was analysed using a non-linear regression analysis of the normalized response in GraphPad Prism version 7.04.

The *in vitro* elastase (Athens Research and Technology) inhibition assay was performed in 0.1 M Tris-HCl, pH 8.1, 0.02 M $CaCl_2$. Each well was incubated with 25 μL elastase solution in buffer (final concentration, 186 nM) and 25 μL inhibitor solution (final concentration ranging from 0.12 μM to 31.25 μM) for 15 min at 37 °C before addition of 100 μL of methoxysuccinyl-Ala-Ala-Pro-Val-pNA (Sigma-Aldrich) substrate. The inhibitor solution was prepared by diluting the 1 mg/mL stock solution in DMSO with buffer, and the resulting solution was then serially diluted to acquire eight concentration levels. The final concentration of DMSO in the well containing the highest inhibitor concentration did not exceed 1%. The 1 mg/mL substrate solution was prepared in 1% DMSO in buffer to fully solubilize the substrate. All experiments were conducted in triplicate and the residual activity of the enzyme in each well was measured by absorbance at 405 nm every 20 s for 10 min. IC_{50}

values were obtained based on a nonlinear regression of a normalized variable slope (four-parameter) model [56].

For data analysis, the percentages of the enzyme activity remaining at each level of an inhibitor concentration was calculated in reference to the free enzyme (100% enzyme activity) and media controls (0% enzyme activity). The concentrations of inhibitors and the percentages of remaining protease activity calculated are then inserted into the Prism. Results obtained from these experiments are presented in the Supporting *Information*.

4.2.2. Anti-bacterial cell assays

4.2.2.1. Pseudomonas aeruginosa assay. P. aeruginosa strain PAO1 was cultured overnight by shaking at 37 °C in fluorescent broth (FB) and diluted 1/1000 in 10 mL with 60 μL of 1 M $MgSO_4$ added. Separately, 6 and 12 μL of 10 mM stock solutions (diluted in DMSO) of the protease inhibitors **JO146**, **2**, and **3** were added to 1.2 mL of cellular dilutions, resulting in 50 μM and 100 μM final concentrations. Controls had 6 μL (0.5%) and 12 μL (1%) DMSO added. 5 × 200 μL of the 1.2 mL solutions were added to a 96-well black clear bottom plate. Growth (OD 600) and fluorescence ([Ex] 405 nm/[Em] 460 nm) were measured every 15 min for 24 h or 48 h. Pyoverdine, a fluorescent biomolecule, produced by the bacteria was analysed as area under the curve (AUC) as a biomarker for *P. aeruginosa* growth [57]. FB (pH 7.0) consisted of 10 g/L bacto™ tryptone (peptone 140), 10 g/L bacto protease peptone #3 (peptone 180), 18.6 mM K_2HPO_4, and 1% (v/v) glycerol.

4.2.2.2. Staphylococcus aureus and Escherichia coli assays. S. aureus, and *E. coli* were grown in cation adjusted Mueller Hinton (MH) broth at 37 °C with shaking (200 rpm). MIC plates were set up as follows; 150 μL of Ca-MH media was added to column 1 (A-H) and 75 μl of media was added to the remaining wells of a 96-well plate. Compound was added to column 1 at a final concentration of 32 μg/mL (approximately 50 μM) and serially diluted 2-fold (75 μL transfer) into the neighbouring wells, making sure to discard 75 μL from the last well. Thus, resulting in a serial dilution of each compound from 32 μg/mL to 0.015 μg/mL (0.0025 μM). Overnight cultures of bacteria were diluted in fresh Ca-MH before adding 75 μL of culture to each well of the MIC plate, to achieve a uniform CFU/ml of ~5×10^5 in the MIC plate. Plates were incubated at 37 °C with shaking for 24 h before determining the MIC. MIC's were determined as the lowest concentration at which growth did not occur. Assays were carried out in technical triplicate.

4.2.2.3. Chlamydia trachomatis and Chlamydia pecorum cell assays. In vitro C. trachomatis and *C. pecorum* cell culture assays were conducted according to our previously reported method [17]. *C. trachomatis* D (D/UW-3/Cx; CtD) and *C. pecorum* G (MC/MarsBar; CpG) isolates were routinely cultured in HEp-2 cells and McCoy B cells, respectively, in high glucose (4.5 g/L) DMEM (product number D6546, Sigma-Aldrich) supplemented with heat-inactivated 10% foetal calf serum (Sigma-Aldrich), 4 mM L-Alanyl-L-glutamine, 100 μg/mL streptomycin, and 50 μg/mL gentamicin. Inhibition experiments were routinely conducted in 96-well plates seeded with 20,000 host cells per well 24 h prior to the chlamydial infection. A high Multiplicity of Infection (MOI) of 12 for *C. trachomatis* and MOI of 4 for *C. pecorum* was used to achieve a high concentration of infectious yield, to allow for more accurate determination of the dynamic range of responses to each compound at each dose. Infections were synchronised at 500×*g*/28 °C for 30 min, and infectious media was replaced with fresh supplemented DMEM containing 1 μg/mL cycloheximide at 2 h post infection (PI). Cultures were treated with a dose series of 25 μM, 50 μM and 100 μM of each compound at 16 h PI, alongside 1% v/v DMSO and media-only controls. Each treatment was performed in triplicate. At 44 h PI, cells were harvested via vigorous pipette-lysis and serially diluted onto fresh host cell monolayers, which were fixed and stained at 44 h PI for enumeration of infectious yield.

4.2.3. Cytotoxicity assessments against human epithelial monolayers

4.2.3.1. MTS assay for cell metabolism and proliferation. MTS assays were performed using CellTiter 96® AQueous MTS Reagent Powder (Promega, Australia) according to the manufacturer's instructions. MTS powder and phenazine methosulfate (PMS; Sigma, USA) were solubilised in dPBS and filter sterilised before use.

HEp-2 cells were cultured at a density of 5000 cells/well and at 24 h post-culture were treated with 1% v/v DMSO and inhibitors (at 25 μM and 100 μM doses); media only controls were also included, with all treatments performed in triplicate. At 24 h following treatment, the cells were given fresh supplemented DMEM and incubated with MTS/PMS solution for 4 h prior to reading the absorbance at 490 nm. Following absorbance readings, all media was removed. Data was statistically analysed in GraphPad Prism 7.

4.2.3.2. LDH assay for cell integrity. Extracellular lactate dehydrogenase (LDH) was measured in treated HEp-2 cells using CytoTox 96® Non-Radioactive Cytotoxicity Assay (Promega, Australia) according to the manufacturer's instructions. HEp-2 cells were cultured at a density of 5000 cells/well to match the MTS assay. At 24 h post-culture, cells were treated with 25 μM and 100 μM of each **JO146** analogue, including 1% v/v DMSO and media only controls, each performed in triplicate. Cells were treated for 8 h prior to removal of supernatant. Maximum release controls were also performed 45 min prior to supernatant removal, where untreated cells were lysed with 0.8% v/v Triton X-100. Cell supernatants were treated with CytoTox reagent for 30 min followed by stop solution, as per manufacturer's instructions. The absorbance of each well was then read at 490 nm. Statistical analysis of data was performed in GraphPad Prism 7.

4.3. Docking studies

Docking was conducted using Gold v5.2 with a previously constructed homology model of CtHtrA [51]. Ligands were drawn using Avogadro® and docked as covalent ligands (to Ser197) using the CHEMPLP scoring function. Two key hydrogen bonding constraints between the enzyme and ligands were pre-defined between C═O of Thr213 and NH of P1 amide, and between NH of Ile215 amide and C═O of 2-pyridone, which corresponds to the C═O of P3 in peptide-based analogues. These constraints were predefined to enable direct comparison with the docking position of the peptidic lead compound **JO146**, and as these hydrogen bonds had been previously verified by X-ray crystallography of HNE complexed with 5-aminopyrimidin-6-one-containing trifluoromethyl ketones inhibitors (PDB 1EAT) [58].

Declaration of competing interest

The authors have no conflicts of interest.

Acknowledgments

This project has been supported by the NSW Government under the NSW Koala Strategy. Jimin Hwang was supported by a University of Otago Doctoral Scholarship. Natalie Strange was supported by a UTS Faculty of Science HDR (Higher Degree by Research) Scholarship. The authors would like to thank the Department of Chemistry at the University of Otago for use of their NMR and mass spec facilities.

Appendix A. Supplementary data

Supplementary data to this article can be found online at https://doi.org/10.1016/j.ejmech.2021.113692.

References

[1] L. Newman, J. Rowley, S. Vander Hoorn, N.S. Wijesooriya, M. Unemo, N. Low, G. Stevens, S. Gottlieb, J. Kiarie, M. Temmerman, PloS One 10 (2015), e0143304 e0143304.
[2] M. Mohammadpour, M. Abrishami, A. Masoumi, H. Hashemi, J. Curr. Ophthalmol. 28 (2016) 165–169.
[3] A.I. Zambrano, S. Sharma, K. Crowley, L. Dize, B.E. Muñoz, S.K. Mishra, L.A. Rotondo, C.A. Gaydos, S.K. West, PLoS Neglected Trop. Dis. 10 (2016), e0005003 e0005003.
[4] A. Upton, L. Bissessor, P. Lowe, X. Wang, G. McAuliffe, Sex. Health 15 (2018) 232–237.
[5] M. Unemo, W.M. Shafer, Clin. Microbiol. Rev. 27 (2014) 587–613.
[6] A.W. Kimberly, A.B. Gail, MMWR. Recommendations and reports 64 (2015) 1–137.
[7] O. Forslund, M. Hjelm, R. El-Ali, A. Johnsson, C. Bjartling, Acta Derm. Venereol. 97 (2017) 1235–1238.
[8] C. McAlpine, D. Lunney, A. Melzer, P. Menkhorst, S. Phillips, D. Phalen, W. Ellis, W. Foley, G. Baxter, D. de Villiers, R. Kavanagh, C. Adams-Hosking, C. Todd, D. Whisson, R. Molsher, M. Walter, I. Lawler, R. Close, Biol. Conserv. 192 (2015) 226–236.
[9] B. Markey, C. Wan, J. Hanger, C. Phillips, P. Timms, Vet. Microbiol. 120 (2007) 334–342.
[10] J.E. Griffith, D.P. Higgins, K.M. Li, M.B. Krockenberger, M. Govendir, J. Vet. Pharmacol. Therapeut. 33 (2010) 595–604.
[11] A. Robbins, J. Loader, P. Timms, J. Hanger, PloS One 13 (2018), e0209679 e0209679.
[12] J. Skórko-Glonek, D. Figaj, U. Zarzecka, T. Przepiora, J. Renke, B. Lipinska, Curr. Med. Chem. 24 (2017) 2174–2204.
[13] M. Löwer, T. Geppert, P. Schneider, B. Hoy, S. Wessler, G. Schneider, PloS One 6 (2011), e17986.
[14] A. M. Perna, T. Rodrigues, T. P. Schmidt, M. Bohm, K. Stutz, D. Reker, B. Pfeiffer, K. H. Altmann, S. Backert, S. Wessler and G. Schneider, Angew. Chem., 54, 10244-10248.
[15] N. Tegtmeyer, Y. Moodley, Y. Yamaoka, S.R. Pernitzsch, V. Schmidt, F.R. Traverso, T.P. Schmidt, R. Rad, K.G. Yeoh, H. Bow, J. Torres, M. Gerhard, G. Schneider, S. Wessler, S. Backert, Mol. Microbiol. 99 (2016) 925–944.
[16] S. Gloeckl, V.A. Ong, P. Patel, J.D.A. Tyndall, P. Timms, K.W. Beagley, J.A. Allan, C.W. Armitage, L. Turnbull, C.B. Whitchurch, M. Merdanovic, M. Ehrmann, J.C. Powers, J. Oleksyszyn, M. Verdoes, M. Bogyo, W.M. Huston, Mol. Microbiol. 89 (2013) 676–689.
[17] A. Lawrence, T. Fraser, A. Gillett, J.D.A. Tyndall, P. Timms, A. Polkinghorne, W.M. Huston, Sci. Rep. 6 (2016) 31466.
[18] S. Backert, S. Bernegger, J. Skórko-Glonek, S. Wessler, Cell Microbiol. 20 (2018), e12845 n/a.
[19] K. Ohmoto, T. Yamamoto, M. Okuma, T. Horiuchi, H. Imanishi, Y. Odagaki, K. Kawabata, T. Sekioka, Y. Hirota, S. Matsuoka, H. Nakai, M. Toda, J.C. Cheronis, L.W. Spruce, A. Gyorkos, M. Wieczorek, J. Med. Chem. 44 (2001) 1268–1285.
[20] J. Gising, A.K. Belfrage, H. Alogheli, A. Ehrenberg, E. Åkerblom, R. Svensson, P. Artursson, A. Karlén, U.H. Danielson, M. Larhed, A. Sandström, J. Med. Chem. 57 (2014) 1790–1801.
[21] P.E.J. Sanderson, K.J. Cutrona, B.D. Dorsey, D.L. Dyer, C.M. McDonough, A.M. Naylor-Olsen, I.W. Chen, Z. Chen, J.J. Cook, S.J. Gardell, J.A. Krueger, S.D. Lewis, J.H. Lin, B.J. Lucas, E.A. Lyle, J.J. Lynch, M.T. Stranieri, K. Vastag, J.A. Shafer, J.P. Vacca, Bioorg. Med. Chem. Lett 8 (1998) 817–822.
[22] C.S. Burgey, K.A. Robinson, T.A. Lyle, P.E.J. Sanderson, S.D. Lewis, B.J. Lucas, J.A. Krueger, R. Singh, C. Miller-Stein, R.B. White, B. Wong, E.A. Lyle, P.D. Williams, C.A. Coburn, B.D. Dorsey, J.C. Barrow, M.T. Stranieri, M.A. Holahan, G.R. Sitko, J.J. Cook, D.R. McMasters, C.M. McDonough, W.M. Sanders, A.A. Wallace, F.C. Clayton, D. Bohn, Y.M. Leonard, T.J. Detwiler, J.J. Lynch, Y. Yan, Z. Chen, L. Kuo, S.J. Gardell, J.A. Shafer, J.P. Vacca, J. Med. Chem. 46 (2003) 461–473.
[23] M.S. South, T.A. Dice, T.J. Girard, R.M. Lachance, A.M. Stevens, R.A. Stegeman, W.C. Stallings, R.G. Kurumbail, J.J. Parlow, Bioorg. Med. Chem. Lett 13 (2003) 2363–2367.
[24] J.J. Parlow, B.L. Case, T.A. Dice, R.L. Fenton, M.J. Hayes, D.E. Jones, W.L. Neumann, R.S. Wood, R.M. Lachance, T.J. Girard, N.S. Nicholson, M. Clare, R.A. Stegeman, A.M. Stevens, W.C. Stallings, R.G. Kurumbail, M.S. South, J. Med. Chem. 46 (2003) 4050–4062.
[25] J.J. Parlow, R.G. Kurumbail, R.A. Stegeman, A.M. Stevens, W.C. Stallings, M.S. South, J. Med. Chem. 46 (2003) 4696–4701.
[26] D.S. Osman, A.S. James, K.S. Anita, M.L. Rhonda, J.P. John, S.S. Michael, S.W. Rhonda, S.N. Nancy, J. Pharmacol. Exp. Therapeut. 306 (2003) 1115–1121.
[27] P.S. Dragovich, T.J. Prins, R. Zhou, T.O. Johnson, E.L. Brown, F.C. Maldonado, S.A. Fuhrman, L.S. Zalman, A.K. Patick, D.A. Matthews, X. Hou, J.W. Meador, R.A. Ferre, S.T. Worland, Bioorg. Med. Chem. Lett 12 (2002) 733–738.
[28] P.S. Dragovich, T.J. Prins, R. Zhou, E.L. Brown, F.C. Maldonado, S.A. Fuhrman, L.S. Zalman, T. Tuntland, C.A. Lee, A.K. Patick, D.A. Matthews, T.F. Hendrickson, M.B. Kosa, B. Liu, M.R. Batugo, J.-P.R. Gleeson, S.K. Sakata, L. Chen, M.C. Guzman, J.W. Meador, R.A. Ferre, S.T. Worland, J. Med. Chem. 45 (2002) 1607–1623.
[29] L.L. Zhang, Daizong, Xinyuanyuan Sun, Ute Curth, Christian Drosten, Sauerhering, S.B.R. Lucie, Katharina Rox Becker, Rolf Hilgenfeld, Science 368 (2020) 409–412.
[30] E. Verissimo, N. Berry, P. Gibbons, M.L.S. Cristiano, P.J. Rosenthal, J. Gut, S.A. Ward, P.M. O'Neill, Bioorg. Med. Chem. Lett 18 (2008) 4210–4214.
[31] A.A. Agbowuro, J. Hwang, E. Peel, R. Mazraani, A. Springwald, J.W. Marsh, L. McCaughey, A.B. Gamble, W.M. Huston, J.D.A. Tyndall, Biorg. Med. Chem. 27 (2019) 4185–4199.
[32] I. Schechter, A. Berger, Biochem. Biophys. Res. Commun. 27 (1967) 157–162.
[33] V. Natarajan, K. Byeang, Curr. Med. Chem. 9 (2002) 2243–2270.
[34] D.A. Matthews, R.A. Alden, J.J. Birktoft, S.T. Freer, J. Kraut, J. Biol. Chem. 250 (1975) 7120.
[35] P.C. Weber, S.-L. Lee, F.A. Lewandowski, M.C. Schadt, C.-H. Chang, C.A. Kettner, Biochemistry (Easton) 34 (1995) 3750–3757.
[36] M.R. Angelastro, S. Mehdi, J.P. Burkhart, N.P. Peet, P. Bey, J. Med. Chem. 33 (1990) 11–13.
[37] A. Poliakov, A. Sandström, E. kerblom, U. Helena Danielson, J. Enzym. Inhib. Med. Chem. 22 (2007) 191–199.
[38] B.E. Maryanoff, M.J. Costanzo, Biorg. Med. Chem. 16 (2008) 1562–1595.
[39] A. Lentini, F. Farchione, B. Ternai, N. Kreua-Ongarjnukool, P. Tovivich, Biol. Chem. 368 (1987) 369–378.
[40] A.D. Pehere, A.D. Abell, Tetrahedron Lett. 52 (2011) 1493–1494.
[41] Y. Basel, A. Hassner, J. Org. Chem. 65 (2000) 6368.
[42] P. Warner, R.C. Green, B. Gomes, A.M. Strimpler, J. Med. Chem. 37 (1994) 3090–3099.
[43] B. Li, S. Cai, D.-M. Du, J. Xu, Org. Lett. 9 (2007) 2257–2260.
[44] M. Hopper, T. Gururaja, T. Kinoshita, J.P. Dean, R.J. Hill, A. Mongan, J. Pharmacol. Exp. Therapeut. 372 (2020) 331.
[45] S. Venkatraman, S.L. Bogen, A. Arasappan, F. Bennett, K. Chen, E. Jao, Y.-T. Liu, R. Lovey, S. Hendrata, Y. Huang, W. Pan, T. Parekh, P. Pinto, V. Popov, R. Pike, S. Ruan, B. Santhanam, B. Vibulbhan, W. Wu, W. Yang, J. Kong, X. Liang, J. Wong, R. Liu, N. Butkiewicz, R. Chase, A. Hart, S. Agrawal, P. Ingravallo, J. Pichardo, R. Kong, B. Baroudy, B. Malcolm, Z. Guo, A. Prongay, V. Madison, L. Broske, X. Cui, K.-C. Cheng, Y. Hsieh, J.-M. Brisson, D. Prelusky, W. Korfmacher, R. White, S. Bogdanowich-Knipp, A. Pavlovsky, P. Bradley, A.K. Saksena, A. Ganguly, J. Piwinski, V. Girijavallabhan, F.G. Njoroge, J. Med. Chem. 49 (2006) 6074–6086.
[46] Ł. Winiarski, J. Oleksyszyn, M. Sieńczyk, J. Med. Chem. 55 (2012) 6541–6553.
[47] T. Maxson, D.A. Mitchell, Tetrahedron 72 (2016) 3609–3624.
[48] L.O. Eckert, R.J. Suchland, S.E. Hawes, W.E. Stamm, J. Infect. Dis. 182 (2000) 540–544.
[49] OECD, Test No. 491: Short Time Exposure in Vitro Test Method for Identifying I) Chemicals Inducing Serious Eye Damage and Ii) Chemicals Not Requiring Classification for Eye Irritation or Serious Eye Damage, OECD Publishing, Paris, 2020. Paris.
[50] i. b. International, Organization for Standardization, *Biological Evaluation of Medical Devices. Part 5, Tests For in Vitro Cytotoxicity* ISO, third ed., 2009. Geneva.
[51] S. Gloeckl, J.D.A. Tyndall, S.H. Stansfield, P. Timms, W.M. Huston, J. Mol. Microbiol. Biotechnol. 22 (2012) 10–16.
[52] Y. Odagaki, K. Ohmoto, S. Matsuoka, N. Hamanaka, H. Nakai, M. Toda, Y. Katsuya, Biorg. Med. Chem. 9 (2001) 647–651.
[53] P. Mendez-Samperio, Infect. Drug Resist. 7 (2014) 229.
[54] W.M. Huston, J.E. Swedberg, J.M. Harris, T.P. Walsh, S.A. Mathews, P. Timms, FEBS Lett. 581 (2007) 3382–3386.
[55] W.M. Huston, J.D.A. Tyndall, W.B. Lott, S.H. Stansfield, P. Timms, PloS One 6 (2011), e24547.
[56] J.M. Strelow, SLAS Discovery 22 (2017) 3–20.
[57] X. Mulet, G. Cabot, A.A. Ocampo-Sosa, M.A. Domínguez, L. Zamorano, C. Juan, F. Tubau, C. Rodríguez, B. Moyà, C. Peña, L. Martínez-Martínez, A. Oliver, D. Spanish Network for Research in Infectious, Antimicrob. Agents Chemother. 57 (2013) 5527–5535.
[58] C.A. Veale, P.R. Bernstein, C. Bryant, C. Ceccarelli, J.R. Damewood Jr., R. Earley, S.W. Feeney, B. Gomes, B.J. Kosmider, J. Med. Chem. 38 (1995) 98–108.